# The Internal Space and Boundary Growth of the Spectre and Tsiokos's Chair44 Tilings

Brent Hartshorn and Tristan Romanov

October 26, 2026

**Abstract**

The planar Spectre and Tsiokos's three-dimensional Chair44 are aperiodic monotiles whose tilings are hierarchical; they are compared here by exact computation. The Spectre inflates by the unit $\lambda^2 = \sqrt{15}+4$ of $\mathbb{Z}[\sqrt{15}]$. Its supertile perimeter is $2F_{3k+5}+4$ at every order $k$, proved by a finite exact certificate, so it grows by the unit $2+\sqrt{5}$ of $\mathbb{Q}(\sqrt{5})$, faster than the linear inflation. The boundary of the limiting supertile is a fractal of box dimension $\log(2+\sqrt{5})/\log\lambda$, and the tail of the common-ancestor levels of neighbouring tiles decays exactly by $\nu/\lambda^2$. The inflation acts on the vertex module $\mathbb{Z}^4$ with two expanding and two contracting directions, and the internal plane is given exactly; the window is the attractor of contracting similarities, with boundary dimension $\log(5+2\sqrt{6})/\log(4+\sqrt{15})$. The Chair44 inflates by the integer 2 on $\mathbb{Z}^3$, with no Euclidean internal space (its internal space is 2-adic) and no twist; its centre set, that of the classical three-dimensional chair, has an explicitly computed pure-point diffraction measure. The main result is that every lattice-registered tiling obeying the 44 contact rules lies in the substitution hull, and that its symmetry group is conjugate to one of 1, $C_2$ (a half-turn about a face diagonal), $C_4$ and $D_4$. Both statements use Kamenetsky's unique-hierarchy criterion, whose finite certificate is checked here independently, and they transfer to every tiling by the Chair44 solid through Tsiokos's registration theorem, which has been audited but not refereed. Orientation sums and contact matrices separate the two tilings. Four finite-patch computations then test whether the Spectre's substitution hierarchy can serve as a clock: positional clustering shows no arrow, the radius needed to recognize an ancestor grows about threefold per level without making one, the look-back law is shared with a quadtree, and the parity flip of the construction shows in the outlines of supertiles and not in the tiles.

## 1 Introduction

A tiling that exists only by inflation carries an arithmetic: the number by which it inflates, the field that number generates, and what that field leaves behind. The Spectre of Smith, Myers, Kaplan and Goodman-Strauss [1, 2] inflates by a unit of a real quadratic field, and the Chair44 of Tsiokos [4] by the integer 2. The Spectre's vertices lie in $\mathbb{Z}[\zeta_{12}]$, a module of rank four, on which the inflation acts as an integer matrix with eigenvalues $\pm\lambda$ and $\pm\lambda^{-1}$: the two contracting directions form an internal space in which the vertices fill a bounded window. An integer inflation $m > 1$ acts as $mI$, nothing contracts, and the internal space is $m$-adic. This paper computes that difference exactly.

A companion note [3] states the physical hypothesis that motivated this work; nothing here depends on it. Statements are stratified. *Facts* are exact statements: each is proved, or verified by an exact finite computation and then stated only for the range computed, or quoted, and

the text says which; the supplement lists every Fact with the method by which it was obtained. *Propositions* are computations with a modelling step, and *Theorems*, *Lemmas* and *Corollaries* carry proofs. Results labelled *computation, not Fact* are numerical, on finite patches, and enter no ledger.

The Spectre is analysed in Sections 2–4 (substitution matrix, spectrum, marginal charges), 5 (perimeter growth) and 6 (four-dimensional lift), the Chair44 in Sections 7 and 8, with a proof, resting on two quoted inputs, that every Chair44 tiling lies in the substitution hull and a classification of the symmetry groups of its tilings in Section 7.4, and the two are compared in Section 9. Section 10 tests whether the Spectre's substitution hierarchy can serve as a clock.

What is not claimed matters as much. The inputs are these. For the Spectre: the published substitution rule of [2], that is, the matrix (1) together with the placement transforms of the construction, from which every placed patch is built. For the Chair44: Tsiokos's solid and its eight substitution children [4]. The einstein property of the Chair44 is Tsiokos's claimed proof [4], quoted. The hull theorem of Section 7.4 is proved for tilings obeying the contact rules, using Kamenetsky's unique-hierarchy criterion [12] with its finite certificate checked independently (Lemma 1), and for the solid it rests in addition on Tsiokos's registration theorem [4], quoted; that proof has been audited by the second author [7] but has not been refereed. That the Spectre diffraction is pure point is a published theorem [8, 9], not re-proved here, and the centre set of the Chair44 is that of the classical three-dimensional chair [13, 15]. Section 11 lists the rest.

## 2 Exact Spectral Theory of the Spectre Monotile Substitution

Figure 1 summarises the substitution that this section analyses.

The substitution acts on nine species ($\Gamma$, $\Delta$, $\Theta$, $\Lambda$, $\Xi$, $\Pi$, $\Sigma$, $\Phi$, $\Psi$), with $\Gamma$ carrying the Mystic pair $\Gamma_1 + \Gamma_2$, $\Gamma_2 = \mathrm{Tile}(b, a)$. The matrix is transcribed from the published rule [2]; every statement of Sections 2–4 that does not mention placed tiles is derived from it alone.

$$M = \begin{pmatrix} 1 & 1 & 1 & 1 & 1 & 1 & 1 & 1 & 1 \\ 1 & 1 & 1 & 1 & 1 & 1 & 1 & 1 & 1 \\ 1 & 0 & 0 & 0 & 0 & 0 & 0 & 0 & 0 \\ 0 & 0 & 0 & 0 & 0 & 0 & 1 & 0 & 0 \\ 1 & 2 & 0 & 1 & 0 & 1 & 2 & 0 & 0 \\ 1 & 1 & 2 & 1 & 1 & 0 & 1 & 1 & 0 \\ 1 & 1 & 1 & 1 & 1 & 1 & 1 & 1 & 1 \\ 1 & 2 & 2 & 2 & 2 & 2 & 1 & 2 & 2 \\ 0 & 0 & 1 & 1 & 2 & 2 & 0 & 2 & 3 \end{pmatrix} \tag{1}$$

**Fact 1** (Inflation factor and its arithmetic)**.** *The Perron eigenvalue is $\lambda^2 = \sqrt{15} + 4$, the fundamental unit of $\mathbb{Z}[\sqrt{15}]$: $4^2 - 15 \cdot 1^2 = 1$ is the least Pell solution. The linear inflation factor is*

$$\lambda = \sqrt{\sqrt{15} + 4} = \tfrac{1}{2}(\sqrt{6} + \sqrt{10}) = 2.8058837\ldots, \qquad (\lambda - \lambda^{-1})^2 = 6, \qquad (\lambda + \lambda^{-1})^2 = 10,$$

*with minimal polynomial $x^4 - 8x^2 + 1$ and splitting field $\mathbb{Q}(\sqrt{6}, \sqrt{10})$. The two channel identities are proved in $\mathbb{Z}[\sqrt{15}]$ without evaluating a square root: each is $\lambda^2 + \lambda^{-2} \mp 2$, and the $\sqrt{15}$ parts cancel. Tile counts, and with them supertile areas, therefore grow by the factor $\lambda^2$ per level.*

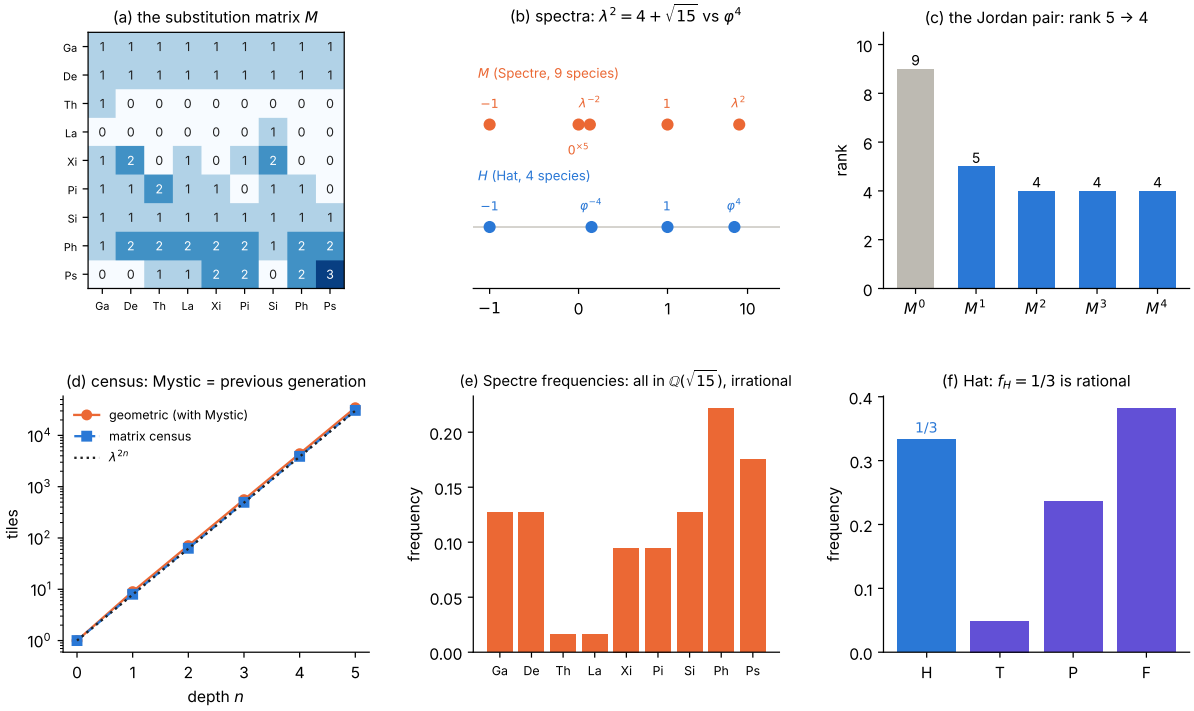


Figure 1: The substitution. (a) The matrix $M$. (b) Its spectrum on a symmetric logarithmic axis, against that of the Hat matrix: the Pisot pair $\lambda^{\pm 2}$ with $\lambda^2 = 4 + \sqrt{15}$, and $\varphi^{\pm 4}$. (c) The ranks of $M^n$ drop from 5 to 4 and stay: the Jordan pair. (d) Tiles by depth, with and without the Mystic, against $\lambda^{2n}$. (e,f) The species frequencies: irrational for the Spectre, with the Hat's $f_H = 1/3$ rational.

**Fact 2** (Transfer spectrum: a Jordan pair among the zero modes)**.** $\chi_M(x) = x^5(x-1)(x+1)(x^2-8x+1)$, *and the zero sector carries structure the spectrum alone does not show:*

$$\operatorname{rank} M = 5, \qquad \operatorname{rank} M^n = 4 \quad (n \geq 2).$$

*The zero eigenvalue has algebraic multiplicity five and geometric multiplicity four, so $M$ is not diagonalizable: its Jordan blocks at 0 have sizes $1, 1, 1, 2$. The kernel of $M$ has dimension four and that of $M^2$ dimension five, so one census direction survives one substitution and is erased by the second. The remaining spectrum is the Pisot-unit pair $\{\lambda^2, \lambda^{-2}\}$ and two marginal eigenvalues $\pm 1$. Relative to the Perron growth, the Pisot conjugate decays by $\lambda^{-4} = (4-\sqrt{15})^2 \approx 0.0161332$ per step and the marginal modes by $\lambda^{-2}$; so species frequencies converge at the rate $\lambda^{-2}$ whenever a marginal charge of Section 4 is nonzero on the seed (as it is for the seed $\Delta$), and at the rate $\lambda^{-4}$ otherwise. The zero modes are gone after two steps.*

## 3 Matrix Iteration Versus Placed Patch Counts

A patch can be counted two ways and the difference matters, so it is settled here before anything uses it.

The *matrix census* is what iterating (1) produces: nine species, one $\Gamma$ entry, seeded with a single $\Delta$ (the seed of Table 1; seeding with $\Gamma$ gives 7, 55, 433, ...). The *geometric census* is

what a placed patch contains, and a placed patch carries the Mystic as well, so it is larger. The two are not interchangeable.

**Fact 3** (The Mystic is the previous generation)**.** *Row* $\Gamma$ *of* $M$ *is all ones, so* $N_\Gamma(n)$ *is the entire census at depth* $n-1$*; the Mystic is a second copy of it. Hence*

$$T_{\text{geom}}(n) = T(n) + T(n-1),$$

*and both sequences obey* $T(n{+}1) = 8T(n) - T(n{-}1)$*, the recurrence whose characteristic polynomial is the quadratic factor of* $\chi_M$*. The recurrence holds for every seed and every* $n$*: the row of ones satisfies* $\mathbf{1}^\top(M^2 - 8M + I) = 0$*, checked entry by entry, so* $T(n{+}2) - 8T(n{+}1) + T(n) = \mathbf{1}^\top M^n(M^2 - 8M + I)e = 0$ *for every seed vector* $e$*.*

| depth | matrix census | geometric census | Mystic |
|---|---|---|---|
| 0 | 1 | 1 | 0 |
| 1 | 8 | 9 | 1 |
| 2 | 63 | 71 | 8 |
| 3 | 496 | 559 | 63 |
| 4 | 3905 | 4401 | 496 |

Table 1: The two censuses. The fourth column is the third minus the second, and is also the second column one row up — which is Fact 3. Charges are linear forms on the nine-species vector and are evaluated against the matrix column.

## 4 Conserved and Alternating Marginal Charges

**Fact 4** (The marginal charges)**.** *The left eigenvectors for the marginal eigenvalues* $\pm 1$*, in the species order of* (1)*, are*

$$Q_+ = (-3, -1, 0, 0, 1, 1, -2, 1, 2), \qquad Q_- = (-1, -1, 2, 0, 1, -1, 0, 1, 0),$$

*satisfying* $Q_+M = Q_+$ *and* $Q_-M = -Q_-$ *exactly over* $\mathbb{Z}$*. Evaluated on the matrix census of Section 3 at depths one to four,*

$$Q_+ = -1, -1, -1, -1, \qquad Q_- = +1, -1, +1, -1.$$

$Q_+$ *is conserved;* $Q_-$ *alternates.*

**Proposition 1** ($Q_-$ and the parity of the construction)**.** *The construction applies a mirror at every level, so all tiles of a depth-n patch have the same handedness and the common determinant of their placements is* $(-1)^n$*; transcribing the published placement chain into* $\mathbb{Q}(\sqrt{3})$ *affine arithmetic, every determinant is exactly* $\pm 1$*, as it must be. Since* $Q_-$ *is a left eigenvector for* $-1$*,* $Q_-(n) = (-1)^n Q_-(e)$ *for a seed* $e$*. For the seed* $\Delta$*,* $Q_-(\Delta) = -1$ *and the determinant equals* $-Q_-(n)$ *at every depth. This is a coincidence of two alternating sequences and not a way of reading parity from species counts:* $Q_-$ *vanishes on single tiles of the species* $\Lambda$*,* $\Sigma$ *and* $\Psi$*, and hence on the supertiles of those species at every depth.*

**Fact 5** (The generational ledger)**.** *Row* $\Theta$ *of* $M$ *is the indicator of* $\Gamma$ *and row* $\Lambda$ *the indicator of* $\Sigma$*, so*

$$N_\Theta(n) = N_\Gamma(n-1), \qquad N_\Lambda(n) = N_\Sigma(n-1)$$

*hold exactly, not asymptotically: two species are a verbatim copy of an earlier generation.*

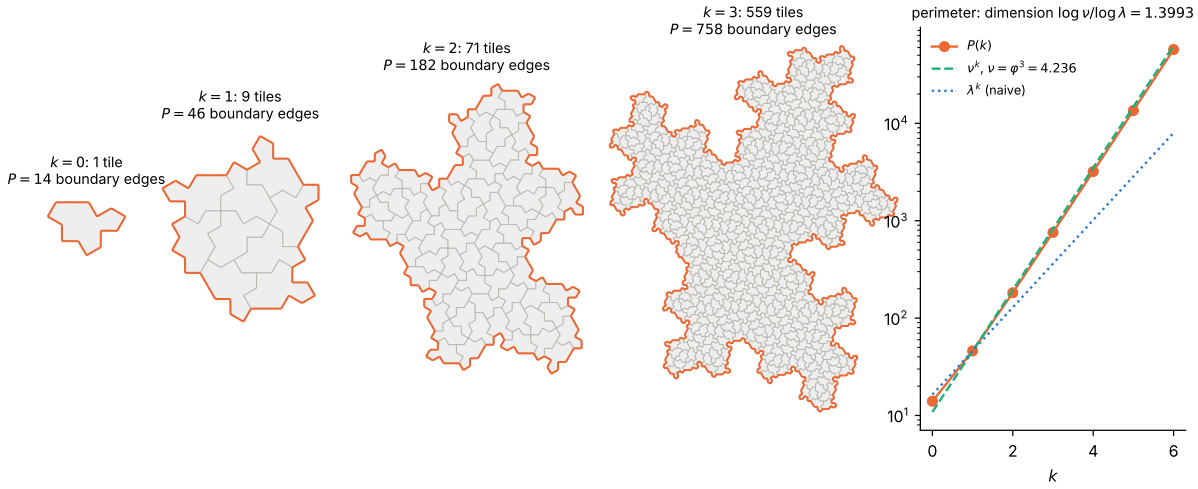


Figure 2: Supertiles of order $k = 0, \ldots, 3$ with their boundary edges (orange), and the perimeter $P(k)$ against $\nu^k$ with $\nu = \varphi^3$ and against the naive $\lambda^k$. The edge counts drawn are counted on the geometry and asserted equal to the recurrence of this section.

### 4.1 The twist of the Spectre supertile

**Fact 6** (The twist of the supertile)**.** *The four key points of a supertile (its quadrilateral) are moved by one level of the construction by a conjugate-linear map $F(w) = D\,\overline{w}$ on $\mathbb{C}^4$, and $B = D\overline{D}$ is complex linear. The quadrilaterals are not similar at any finite level: their corners lie in $\mathbb{Q}(\sqrt{3}, i)$, so squared side lengths lie in $\mathbb{Q}(\sqrt{3})$, which does not contain $\lambda^2$. They become similar in the limit: along the dominant eigenline of $B$, consecutive quadrilaterals are related by the ratio $\lambda$ and a rotation of $-\theta_S$ on even levels and $+\theta_S$ on odd ones, with a relative correction that decays by $\lambda^{-2}$ per level, where*

$$\tan\theta_S = \frac{5\sqrt{3}-6}{13}, \qquad \cos 2\theta_S = \frac{4+3\sqrt{3}}{10}, \qquad \theta_S = 11.565051\ldots^\circ .$$

*The two-level map $B$ has characteristic polynomial $(x-1)^2(x^2-8x+1)$, which carries the quadratic factor of $\chi_M$, and its dominant eigenvalue is the real number $\lambda^2$: over two levels the limiting quadrilateral is dilated and not rotated.*

The $\sqrt{15}$ enters the limiting one-level factor only through its modulus $\lambda$: the doubled phase $e^{-2i\theta_S} = \frac{1}{10}\big(4+3\sqrt{3}+i(3-4\sqrt{3})\big)$ lies in $\mathbb{Q}(\sqrt{3}, i)$, the field of the hexagonal tile coordinates, while $e^{i\theta_S}$ itself does not, since $\cos\theta_S$ has minimal polynomial $400x^4 - 560x^2 + 169$ over $\mathbb{Q}$, of degree four. The alternation of the sign is the mirror applied at each level. The twist is irrational as an angle: $\cos 2\theta_S$ has minimal polynomial $100x^2 - 80x - 11$, so $2\cos 2\theta_S$ is not an algebraic integer and $e^{2i\theta_S}$ is not a root of unity. This is the contrast drawn with the Chair44 in Section 8.

## 5 The other unit: a boundary operator in $\mathbb{Q}(\sqrt{5})$

Figure 2 shows the supertiles whose perimeter is counted here.

Everything above grades the substitution by area. The perimeter is graded by something else, and the two do not live in the same field.

Let $P(k)$ be the number of unit tile edges on the boundary of an order-$k$ supertile. Reading the child multiset off the substitution table — the eight placement slots are the same for every species, and slot 7 is $\Gamma$ in every rule, while $\Gamma$ alone has a null slot and therefore seven children — and subtracting each glued edge twice gives, with $Q$ the $\Gamma$ perimeter and $G$ the number of edges shared between two *different* children,

$$P(k{+}1) = 7P(k) + Q(k) - 2G(k{+}1), \qquad Q(k{+}1) = 6P(k) + Q(k) - 2G_\Gamma(k{+}1). \tag{2}$$

The coefficients are read from the rule, not fitted to counts, and (2) holds at every order (Theorem 1). Two facts make it small enough to solve. First, all eight non-$\Gamma$ species have the *same* outline at every order, since they place the same child outlines in the same slots; this collapses a nine-type problem to two. Second, the glue decomposes by slot pair into thirteen contact sequences. Ten of them satisfy the recurrence of $P$ from the first order on; the contacts of slots 1–4, 1–7 and 4–7 satisfy it only from $k = 5$ on, their first term being exceptional, so their characteristic polynomial carries an extra factor $x$. What closes the system is a boundary substitution in the form of a finite set of contact types.

**Theorem 1.** *For every $k \geq 0$, $P(k+3) = 5P(k+2) - 3P(k+1) - P(k)$ and $P(k) = 2F_{3k+5} + 4$, where $F_n$ is the Fibonacci number; and $Q(k+3) = 5Q(k+2) - 3Q(k+1) - Q(k)$ for every $k \geq 1$.*

*Proof.* The slot transforms of the construction are $x \mapsto A_i x + M_i q_k$, with fixed $A_i$ and fixed integer $4 \times 16$ matrices $M_i$, where $q_k \in \mathbb{Z}^{16}$ is the quadrilateral of order $k$ and $q_{k+1} = \Phi q_k$. So two placed order-$k$ outlines have a relative placement $x \mapsto Ax + Lq_k$ with $L$ independent of $k$. The length $S(k)$ of their common boundary is the sum, over the pairs of their children, of the same quantity one order down, provided the two have disjoint interiors. Two placements are identified when $Lq_k$ agrees for all $k$; this is decided on $q_0, \ldots, \Phi^5 q_0$, because the minimal polynomial of $q_0$ is $(x^2 - 1)(x^4 - 8x^2 + 1)$. Starting from the sibling pairs, the child pairs close on 93 types. Every other child type is separated at every order: by a radius bound for $k \leq 60$, and by the exact eigen-decomposition of $q_k$ for $k > 60$, with a margin of at least 0.097 in units of the quadrilateral's diagonal. On the 93 types the interior overlap vanishes at order 0, hence at every order by the same sum. So the supertiles are genuine patches; this is proved here, not assumed. The state $(P, Q, S_1, \ldots, S_{93})$ then obeys $V(k+1) = BV(k)$ with a fixed $95 \times 95$ integer matrix $B$. The sequence $e^\top B^k p(B) V(0)$, with $p(x) = x^3 - 5x^2 + 3x + 1$, vanishes for $k < 95$, hence for all $k$ by Cayley–Hamilton; the same argument gives the recurrence of $Q$. The closed form follows because $F_{n+6} = 4F_{n+3} + F_n$ and the seeds agree. The computation is `boundary_certificate/check_spectre_boundary_proof.py`. It works from an independent exact transcription of the construction and does not use the rest of the build. □

**Fact 7.** *For every $k \geq 3$, $P(k) = 5P(k-1) - 3P(k-2) - P(k-3)$ (Theorem 1), with $P = 14, 46, 182, 758, 3198, 13534$ and $P(6) = 57318$ also counted exactly (Fact 8).*

The seed of that recurrence is counted from placed tiles, and the count used a rounding key: two edges were identified when their endpoint coordinates agreed to four decimals. A key of that kind can fail in both directions, by merging edges that differ below the tolerance and splitting edges that agree above it, and nothing inside a floating-point computation bounds the failure — it can only be removed.

**Fact 8.** *The same sequence, recounted with edges identified by* equality *of exact $\mathbb{Q}(\sqrt{3})$ endpoint coordinates and from an independent transcription of the placement chain, agrees at every order*

*computed,* $0 \le k \le 6$. *The rounding key is therefore not load-bearing for any of the boundary results.*

The factorisation of $\chi_\partial$ is not left as a spectral remark. Its quadratic factor applied to the sequence annihilates the growing part and leaves behind the constant belonging to the marginal eigenvalue. By Theorem 1 the identity holds for the perimeters at every order:

**Fact 9.** $P(k+2)-4P(k+1)-P(k) = -16$ *for all* $k \ge 0$. *Together with the seed it is equivalent to the recurrence of Fact 7, and it is the* $+1$ *eigenvalue made arithmetic — the boundary's analogue of* $Q_+$.

**Fact 10.** *The companion matrix of that recurrence — the boundary transfer operator — has characteristic polynomial* $\chi_\partial(x) = (x-1)(x^2-4x-1)$. *The marginal eigenvalue* $+1$ *is a conserved boundary quantity, of the same kind as the* $\pm 1$ *of Section 4.*

**Fact 11.** *The Perron root is* $\nu = 2+\sqrt{5} = \varphi^3 = 4.23606797750$.

So, on the orders computed, the area of a supertile inflates by $\lambda^2 = 4+\sqrt{15}$ and its perimeter by $2+\sqrt{5}$. This is a $\mathbb{Q}(\sqrt{15})$ / $\mathbb{Q}(\sqrt{5})$ divide between area and perimeter of the *same* tile. The supertile boundary is golden although the tiling is not.

Since $P(k) \sim c\,\nu^k$ unit edges bound a supertile of diameter of order $\lambda^k$, and since $\nu > \lambda$ the perimeter outgrows the linear scale with exponent $\log\nu/\log\lambda = 1.39925321391$. That exponent is the box dimension of the limiting outline.

**Theorem 2.** *For each parity* $p$, *the rescaled supertiles* $\lambda^{-k}S_k$ *with* $k \equiv p$ *modulo* 2 *converge in the Hausdorff metric to a compact set* $K_p$ *that is the closure of its interior. The box dimension of* $\partial K_p$ *exists and equals* $\log\nu/\log\lambda$.

*Proof.* Rescaled by $\lambda^{-k}$, the placements of Theorem 1 have translations $M_i q_{k-1}/\lambda^k$, and $q_k = \lambda^k a + (-\lambda)^k b + O(1)$. So on each parity they converge geometrically to similarities of ratio $1/\lambda$, and $\lambda^{-k}S_k$ converges to the attractor $K_p$ of the limiting graph-directed system.

The areas of $\lambda^{-k}S_k$ converge to a positive limit, and area is upper semicontinuous under Hausdorff limits. The children matrix $\left(\begin{smallmatrix}7&1\\6&1\end{smallmatrix}\right)$ has Perron root $\lambda^2$. So $K_p$ has positive area and its pieces overlap in measure zero.

A grandchild of $S$ (slot 3 of slot 7) is separated at every order from every contact it could have outside its supertile, with a margin of 0.267 quadrilateral diagonals. In a Spectre tiling of the plane [1] a ball of that relative radius about it therefore lies in the supertile. So $K_p$ has interior and, since its pieces are dense, it is the closure of its interior.

For the upper bound, every point of $\partial K_p$ is within any $\varepsilon$ of the outline of $\lambda^{-k}S_k$ for large $k$. That outline is covered by the depth-$m$ pieces in contact with a piece of a neighbouring supertile, and there are at most $C\nu^m$ of them: the contact matrix on the 93 types of Theorem 1 has characteristic polynomial $x^{84}(x-1)^3(x+1)^4(x^2-4x-1)$, with $\nu$ a simple dominant root.

For the lower bound, 20 of the types share an edge at every order $k \ge 1$, and they contain an irreducible block of spectral radius $\nu$ that sibling pairs reach. So at least $c\nu^m$ pairs of depth-$m$ pieces of two sibling limit tiles meet, each in a point of both boundaries. A box of side $\lambda^{-m}$ meets boundedly many pieces, because the pieces have area of order $\lambda^{-2m}$ and overlap in measure zero.

The finite inputs are checked by `boundary_certificate/check_spectre_fractal.py`. □

The theorem does not use the self-similar Spectre-type tilings of [9], whose tiles are fractal by construction. The limiting Spectre supertile is a fractal in its own right: it has interior, and its

boundary has box dimension strictly between 1 and 2. The growth is also visible at every finite order: $P(k+3) \geq 4P(k+2)+30$ for every $k$, while $\lambda^2 < 16$ hence $\lambda < 4$, so $P(k+1)/P(k) > 4 > \lambda$ for every $k \geq 2$, and a perimeter argument assuming $P(k) \sim \lambda^k$ is wrong at every order.

### 5.1 A closed form, and the directions of the boundary edges

The recurrence has a closed form in Fibonacci numbers.

**Fact 12.** *The supertile perimeter is $P(k) = 2F_{3k+5}+4$ for every $k \geq 0$, where $F_n$ is the Fibonacci number (Theorem 1).*

It follows from the recurrence by induction, because $F_{n+6} = 4F_{n+3}+F_n$ makes $2F_{3k+5}+4$ satisfy the same recurrence and the seeds agree. It says three things that the recurrence did not. The growth $\nu = \varphi^3$ is one Spectre level multiplying the Fibonacci index by three, which is how the golden unit arises. The marginal eigenvalue $+1$ is the constant 4, so $(P(k)-4)/2$ is every third Fibonacci number. And the third root of $x^2 - 4x - 1$ is $2 - \sqrt{5} = -\varphi^{-3}$, which is negative, so that component alternates in sign with the parity of the level. That is the same parity that flips the determinant of the placement matrix, but any quantity alternating with level parity does so, and this is weak evidence of a link to the chirality channel and is not claimed as one.

The boundary edges also have directions. The fourteen edges of the Spectre point along multiples of 30°. Let $h_j$, $j \in \mathbb{Z}/6$, be half the number of boundary edges of an order-$k$ supertile whose direction is $j \cdot 30°$ modulo 180°, so that $\sum_j h_j = P(k)/2$. Splitting the six classes by parity gives, counted on the placed tiling through $k = 6$,

$$\underbrace{h_0 + h_2 + h_4}_{\text{even}} = F_{3k+4} + 1, \qquad \underbrace{h_1 + h_3 + h_5}_{\text{odd}} = F_{3k+3} + 1, \tag{3}$$

whose sum doubled is $P(k)$. The difference of the two totals is exactly $F_{3k+2}$, which is the amplitude of the $\mathbb{Z}/2$ character in Table 2. The remaining two characters of $\mathbb{Z}/6 = \mathbb{Z}/2 \times \mathbb{Z}/3$ stay bounded: their largest amplitude over $k \leq 6$ is 3.61. The group $\mathbb{Z}/6$ is the one that acts on the hexagonal directions of the tiling, and the data identify the group, not the action.

Table 2: Boundary edges of an order-$k$ supertile by direction modulo 180°. Even and odd are the class totals of (3); $|\hat{h}|$ is the largest amplitude of the $\mathbb{Z}/3$ and faithful characters of the folded histogram. Counted on the placed tiling (`chair44_spectre_link.py`); the $k = 6$ row took 66 s. The $P(k)$ column is the recurrence sequence and agrees with the exact count of Fact 8.

| $k$ | $P(k)$ | even | odd | even − odd | $\lvert\hat{h}\rvert$ |
|---|---|---|---|---|---|
| 0 | 14 | 4 | 3 | 1 | 1.00 |
| 1 | 46 | 14 | 9 | 5 | 1.00 |
| 2 | 182 | 56 | 35 | 21 | 2.65 |
| 3 | 758 | 234 | 145 | 89 | 2.65 |
| 4 | 3198 | 988 | 611 | 377 | 3.61 |
| 5 | 13534 | 4182 | 2585 | 1597 | 3.61 |
| 6 | 57318 | 17712 | 10947 | 6765 | 1.73 |

**Counted, not derived.** The closed form and the recurrence are proved for every order (Theorem 1); the split (3) is a count and is not proved beyond $k = 6$. What is proved is the

arithmetic that ties it to the closed form: $F_{3k+4} + F_{3k+3} + 2 = P(k)/2$. The boundedness of the other characters is an observation. The directions are counted with the fork's own tile builder, so this is a count and not an independent second route.

### 5.2 The balanced exponent

A boundary that grows by $\nu$ per level while the area grows by $\lambda^2$ raises the question of how to weigh the two against each other, and the answer is a single exponent.

**Proposition 2.** *Interfaces at coarseness $c < N$ in a depth-$N$ patch, that is, unit edges shared by two different supertiles of order $N-c$, number $\frac{1}{2}\big((T(c)-N_\Gamma(c))P(N-c)+N_\Gamma(c)Q(N-c)-P(N)\big)$, with $Q$ the Mystic perimeter of (2) and $N_\Gamma(c) = T(c-1)$; so, since $P$ and $Q$ grow like $\nu^k$ (Theorem 1), they grow in $c$ by $\mu = \lambda^2/\nu$. If each such unit edge is thickened to a neighbourhood of width $\delta_c = \delta_0\lambda^{-sc}$ and cross-section $\delta_c^2$, as for a curve in $\mathbb{R}^3$, the exponent making every level carry comparable volume is*

$$s^* = 1 - \frac{\log \nu}{\log \lambda^2} = 0.300373393044. \tag{4}$$

The natural guess $s = 2$, one factor of the unit per level, is wrong, and Section 5 says why: every interface edge is a *unit* tile edge whatever level it sits at, so length does not scale with level and only the population does. Two cautions attach to (4). It is exact but *not algebraic*. The ratio $\log\nu/\log\lambda^2$ is irrational, since $\nu^p = \lambda^{2q}$ with integers $p, q \neq 0$ would put an element of $\mathbb{Q}(\sqrt{5})\setminus\mathbb{Q}$ equal to one of $\mathbb{Q}(\sqrt{15})\setminus\mathbb{Q}$; and an irrational ratio of logarithms of algebraic numbers is transcendental by the Gelfond–Schneider theorem [16]. The thickening that defines $s^*$ is a modelling choice and not a property of the tiling; given it, $s^*$ is exact, since $\nu$ is (Theorem 1). And $s^*$ had to be derived rather than fitted: because the interface count depends on $T(c)$ and on $P(N-c)$ together, a single-exponent fit needs $c$ large and $N-c$ large at once, which no finite patch provides. Fitting one anyway returns values that drift with depth and never settle — and the closed form reproduces those drifting values, which is how we know the drift was the estimator and not the geometry.

### 5.3 What the golden appearance is not

$\varphi^3$ next to the Hat's $\varphi^4$ invites the conjecture that the Spectre's boundary combinatorics *are* the Hat's. They are not.

**Fact 13.** *$x^2-4x-1$ divides neither $\chi_M$ nor $\chi_H(x) = (x-1)(x+1)(x^2-7x+1)$, the characteristic polynomial of the four-metatile substitution of the Hat [1].*

**Fact 14.** *$\varphi^n$ has minimal polynomial $x^2 - L_n x + (-1)^n$ with $L_n$ Lucas ($n \geq 1$). So $x^2-4x-1$ is the minimal polynomial of $\varphi^3$ and $x^2-7x+1$ that of $\varphi^4$: any two powers of $\varphi$ have Lucas quadratics as minimal polynomials, and the resemblance carries no information beyond $\mathbb{Q}(\sqrt{5})$.*

The asymmetry is worth recording: the Spectre's own unit is not golden, since $\chi_M$ contributes the trace 8 and 8 is not a Lucas number. The three operators sit at traces 8, 7 and 4 with norms $+1$, $+1$ and $-1$.

What survives is weaker and true. The ratio $\mu = \lambda^2/\nu$ has minimal polynomial $x^4 + 32x^3 - 46x^2 - 32x + 1$ — degree four, not two — so it lies in the compositum $\mathbb{Q}(\sqrt{3},\sqrt{5})$ and in neither quadratic field alone. Both $\lambda^2$ and $\nu$ are Spectre quantities; the Hat does not enter $\mu$.

## 6 The Spectre monotile in four dimensions

Every edge of the Spectre tiling is a unit vector at a multiple of 30°. Following Chéritat and Ma [11], who lift the tilings by the deformable tiles Tile$(a, b)$ of the Hat family to four dimensions, the even multiples are taken to lie in a first plane and the odd multiples in a second. Write $\omega = e^{i\pi/3}$ and $z = e^{i\pi/6}$. An even edge is $p + q\omega$ and an odd edge is $z(r + s\omega)$ with integers, so walking along edges assigns every vertex a point $(p, q, r, s)$ of $\mathbb{Z}^4$, and the projection $(u, v) \mapsto au + bv$ is the deformation of the tile.

**Fact 15** (The integer lift)**.** *Every vertex of a Spectre patch is a sum of unit vectors at multiples of* 30°*, so it lies in* $\mathbb{Z}[\zeta_{12}]$*, which has the basis* $1, \omega, z, z\omega$*; its coordinates* $(p, q, r, s)$ *in that basis are its lift, which is therefore well defined. On the level-*3 *patch (*3734 *vertices) the vertex differences have rank* 4*, and the physical position is* $a(p + q\omega) + bz(r + s\omega)$*, which is the tiling itself at* $a = b = 1$ *and gives a homogeneous quadratic form in* $(a, b)$ *for the area of a tile.*

**Fact 16** (The inflation as an integer matrix)**.** *The supertile recursion moves four key points of the supertile by rotations through multiples of* 60°*, a mirror and translations built from the points themselves; on* $\mathbb{Z}[\zeta_{12}]$ *each is an integer map, so one level is a* $16 \times 16$ *integer matrix* $\Phi$ *on the four key points. It reproduces the floating-point recursion of the construction for three levels (largest difference* $3 \times 10^{-14}$*), and an independent integer transcription reproduces it exactly for six levels; and*

$$\chi_\Phi(x) = (x-1)^4(x+1)^4\,(x^4 - 8x^2 + 1)^2, \qquad x^4 - 8x^2 + 1 = \big(x^2 - (4+\sqrt{15})\big)\big(x^2 - (4-\sqrt{15})\big),$$

*with roots* $\pm\lambda$*,* $\pm\lambda^{-1}$ *and* $\lambda^2 = \sqrt{15} + 4$*. The key-point vector has minimal polynomial* $(x^2 - 1)(x^4 - 8x^2 + 1)$*, and on the part of its cyclic subspace where* $x^4 - 8x^2 + 1$ *vanishes* $\Phi$ *acts by the companion matrix*

$$\begin{bmatrix} 0 & 0 & 0 & -1 \\ 1 & 0 & 0 & 0 \\ 0 & 1 & 0 & 8 \\ 0 & 0 & 1 & 0 \end{bmatrix},$$

*of determinant* 1 *and trace* 0*.*

The unit $4 + \sqrt{15}$ has norm one, which is why the block is unimodular: two eigenvalues expand $(\pm\lambda)$ and two contract $(\pm\lambda^{-1})$. The negative roots come from the mirror applied at every level; over two levels $\Phi^2$ acts on the expanding pair as the real number $\lambda^2$. The Chair44, by contrast, inflates by $2\,I_3$ on $\mathbb{Z}^3$, of determinant 8: every eigenvalue expands and nothing contracts, so there is no Euclidean internal space; the internal space of the chair is 2-adic (Section 7).

**Fact 17** (The internal plane)**.** *A linear functional of* $(p, q, r, s)$ *has bounded range on the supertile corners exactly when it kills the expanding part (*$\Phi^2 = 4 + \sqrt{15}$*) of every iterate of the key-point vector. Each level mirrors the frame, so the odd iterates are mirrored first; the expanding parts then span two dimensions and the annihilator is the plane*

$$\begin{bmatrix} \frac{5}{11} + \frac{3\sqrt{15}}{11} & \frac{3\sqrt{15}}{11} + \frac{16}{11} & -\frac{5\sqrt{15}}{11} - \frac{12}{11} & 0 \\ \frac{3}{11} + \frac{4\sqrt{15}}{11} & \frac{3}{11} + \frac{4\sqrt{15}}{11} & -\frac{3\sqrt{15}}{11} - \frac{5}{11} & 1 \end{bmatrix}$$

*(rows are functionals on* $(p, q, r, s)$*), with entries in* $\mathbb{Q}(\sqrt{15})$*. It agrees with a plane fitted to the lifted vertices to principal cosines above* $1 - 10^{-6}$*. It is bounded on the patches of one parity of*

*level and its mirror image on the other. The extent of the image, each level taken with its bounded plane, is 9.77 at level* 3 *and 9.84 at level* 4*, while the physical extent grows by a factor 2.89 per level (the inflation factor is 2.8059). The Galois conjugate* $z \mapsto z^5$*, the obvious candidate for the internal space, is not bounded: its extent is 50 at level* 3*.*

The plane is bounded for one frame and its image under the mirror for the next, which is why a single fitted plane cannot serve every level. The alternation is exact, and it makes the window the attractor of contracting maps. The slot maps of the construction use only rotations by multiples of 60° and the mirror. Under that group, $\mathbb{Z}[\zeta_{12}] \otimes \mathbb{R}$ is two copies of one irreducible plane, so it has a one-parameter family of invariant planes, not only the two complex embeddings. The conjugate $z \mapsto z^5$ is equivariant for the 30° rotation as well, and it is not the internal space: the images of the supertile key points under it grow like $\lambda^k$.

**Theorem 3.** *On levels of parity* $p$*, the expanding parts of the eight slot translations span a plane* $E_p$*, and every slot map sends* $E_p$ *to* $E_{p+1}$*. Projected along* $E_p$*, the marginal* ($\pm 1$) *parts of the translations are removed by a fixed shift of the internal origin. What remains is* $\lambda^{-k}\gamma_{i,p}$*. The window* $W$ *of the tile positions, read in the frame of each tile, is the attractor of the graph-directed system*

$$Z_p(S) = \bigcup_i \bar{A}_i^{-1}\Big(\gamma_{i,p} + \lambda^{-1}\bigcup_{S'} Z_{p+1}(S')\Big)$$

*of similarities of ratio* $1/\lambda$*. It is dual to the system of Theorem 2, with shape matrix* $\left(\begin{smallmatrix} 7 & 6 \\ 1 & 1 \end{smallmatrix}\right)$*. Its contact matrix, on* 1192 *types, has characteristic polynomial* $(x-1)^{35}(x+1)^{35}x^{1114}(x^4-10x^2+1)^2$*, and spectral radius* $\sqrt{2}+\sqrt{3}$*. Hence*

$$\dim_B \partial W = \frac{\log(\sqrt{2}+\sqrt{3})}{\log\lambda} = \frac{\log(5+2\sqrt{6})}{\log(4+\sqrt{15})} = 1.110977\ldots$$

*Proof.* The plane, intertwining and coboundary statements are linear algebra on the eigencomponents of $q_0$. They are checked to sixty digits, together with a metric in which every internal map is orthogonal (the even products form a group of order 6). The bottom-up expansion of a tile's internal coordinate is then the stated system. The upper bound counts contact pairs: at depth $m$ there are $O(m(\sqrt{2}+\sqrt{3})^m)$ of them, since the dominant root is double. For the lower bound, 142 types lie on infinite paths of the contact graph, so their pieces meet at every depth. They contain an irreducible block carrying $x^4 - 10x^2 + 1$, reached from sibling pairs. As in Theorem 2, this needs the pieces to overlap in measure zero and the window to be the closure of its interior. Both hold because the Spectre tilings have pure point spectrum and regular windows [9]. The computation is `boundary_certificate/spectre_window.py`. □

Baake, Gähler, Mazáč and Sadun obtain the same value for the self-similar member CASPr of the family, from its orbit separation dimension; they note that it deserves a closer analysis [9]. Theorem 3 derives it for the Spectre's own window from the substitution. The image in the fitted plane is bounded, and its boundary cell count (Figure 3; level-5 patch, holes from finite sampling filled) grows by $2^{1.26}$ and $2^{1.16}$ at the successive halvings of the cell size from 0.2, against $2^1$ for a smooth curve, while the area grows by $2^{1.87}$. The boundary is therefore not a smooth curve; a box count at these resolutions gives about 1.2, against the exact 1.111 of Theorem 3. It is not the dimension $\log\nu/\log\lambda$ of the supertile outline in the physical plane (Section 5). It agrees with the windows of Rauzy type that Baake, Gähler, Mazáč and Sadun obtain [8, 9], who prove that Spectre tilings arise from a 4:2 cut-and-project scheme with such

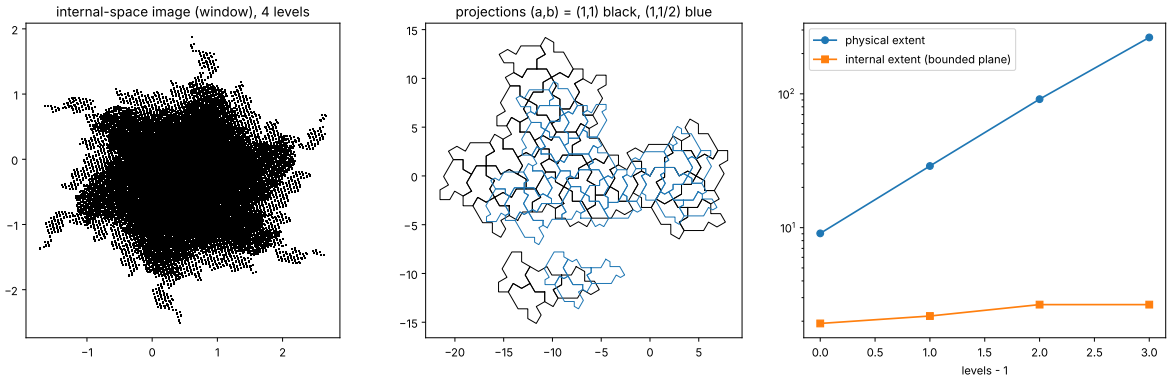


Figure 3: The lift of the Spectre. (a) The internal image of the vertices of a level-4 patch through the exact bounded plane: the window. (b) The projections $(a, b) = (1, 1)$ (black) and $(1, \frac{1}{2})$ (blue) of the same lifted tiles. (c) The physical extent of the lifted patch, which grows with the level, and the internal extent, which does not.

windows; the analogous statement for the Hat family is [10]. Whether anything like this exists for a three-dimensional tile is the question raised by Kamenetsky [12], who finds that the obvious four-dimensional analogues of the Chair44 fail a closure test; the integer inflation of the chair leaves nothing to project.

# 7 From Plane to Bulk: Tsiokos's Chair44

Everything above is two-dimensional; this section asks which of it depends on that. Tsiokos's Chair44 [4] is a candidate three-dimensional einstein, claimed to fill $\mathbb{R}^3$ only aperiodically. The tile is the seven-cube chair (a $2\times2\times2$ block less one corner) with each of its 24 unit faces carrying eight small pyramids of signed heights. Without the pyramids, the substitution of eight chairs on the doubled chair is the classical three-dimensional chair substitution [15, 13]; the decorations select the frames of the children. Its einstein property and strong aperiodicity are Tsiokos's claimed proof, quoted and not checked, and nothing below bears on them. What is recomputed is the combinatorial atlas: `symchair44.py` generates the tile in exact rational arithmetic with no external data and agrees vertex for vertex with the published solid (`symchair44_tests.py`, `chair44_tests.py`); the Facts are in `chair44facts.py` and the supplement.

## 7.1 Combinatorial Reconstruction of the Chair44 Tile

The mesh has 2138 vertices, 6408 edges and 4272 triangles, is a closed manifold of Euler characteristic 2, and has volume exactly 7 for *every* base width $w$ and height unit $h$, because the 192 signed heights sum to zero and the volume is $7 + \frac{4}{3}w^2h\sum_s \gamma_s$. The substitution places eight copies of the chair on the doubled chair, with the refinement $(G, t) \mapsto (GH,\ 2t + Gu)$. There are exactly $3^8 = 6561$ ways to cover the doubled chair by eight rotated chairs; gluing each to depth two and demanding exact complementarity ($\gamma_A + \gamma_B = 0$ for the pyramids on a shared face) leaves four free height classes for 6555 of them and twelve for six. Of those six, three use all 24 orientations and the first in sort order is the published substitution; the selection rule is a convention and is stated as one. The twelve classes are the heights $\pm1, \ldots, \pm12$. The contact

atlas follows from the labels: of 2388 raw face contacts, 1194 are mirror images, 44 are legal, and 30 occur in the depth-three hierarchy, giving 372 site equations of rank 180 and a kernel of dimension 12, the twelve free classes. These counts reproduce the published atlas from the labels alone.

Table 3: The Spectre and the Chair44 side by side. $d$ is the dimension, $\lambda$ the linear inflation, $\nu$ the boundary growth per level, $D_b = \log \nu / \log \lambda$, $s^* = 1 - D_b/d$ and $\mu = \lambda^d/\nu$. The Spectre value of $\nu$ is proved (Theorem 1), and $D_b$ is the box dimension of the boundary of the limiting supertile (Theorem 2). The last two rows are about what is claimed or quoted, not computed.

| | Spectre | Chair44 |
|---|---|---|
| $d$ | 2 | 3 |
| $\lambda$ | $\frac{1}{2}(\sqrt{6}+\sqrt{10}) \approx 2.806$ | 2 |
| tile count per level | $\lambda^2 \approx 7.87$ | $8 = \lambda^3$ |
| boundary growth $\nu$ | $\varphi^3 \approx 4.236$ | 4 |
| $D_b$ | 1.3993 | 2 |
| $s^*$ | 0.3004 | 1/3 |
| $\mu$ | 1.8586 | 2 |
| fractal excess $D_b - (d-1)$ | +0.3993 | 0 |
| area and perimeter fields | $\mathbb{Q}(\sqrt{15})$, $\mathbb{Q}(\sqrt{5})$ | both $\mathbb{Q}$ |
| species, orientations | 9 species, 12 orientations | 24 rotations |
| zero sector | not semisimple | semisimple |
| frequencies | irrational (Pisot) | rational, 1/24 |
| symmetry groups of a tiling | not computed | 1, $C_2^{\text{diag}}$, $C_4$, $D_4$ (Theorem 5) |
| strict chirality | yes, by the tile | yes, by the contacts |
| spectrum of the tiling | pure point [9] | 2-adic, pure point, every atlas tiling (Corollary 2) |

### 7.2 The boundary operator in three dimensions

The Chair44 super-tile of depth $N$ has $24 \cdot 4^N$ boundary faces and $12(8^N - 4^N)$ shared faces, since 24 faces on each of $8^N$ tiles less two for every shared face leaves $24 \cdot 4^N$; the identity holds for all $N$. The faces point equally in all six axis directions, $4^{N+1}$ each, since the chair has four unit faces in each of them; this is the opposite of the Spectre's direction histogram with its golden split. The interface counts obey the form that the law of Proposition 2 takes when there is no Mystic,

$$B_c = \tfrac{1}{2}\big(T(c)P(N-c) - P(N)\big) = 12 \cdot 4^N(2^c - 1), \qquad T(c) = 8^c,\ P(k) = 24 \cdot 4^k,$$

so the interface law is not an accident of the plane. What is different is the exponent. With $\lambda = 2$ and $\nu = 4$ the boundary grows by exactly $\lambda^2$, so $D_b = 2 = d - 1$: the supertile boundary of Tsiokos's Chair44 is an ordinary surface, with no fractal excess, where the Spectre's has +0.3993. Area and perimeter inflate in the same field, so there is no divide between them, and the balanced exponent is the rational $s^* = 1/3$. The separation of the area and perimeter fields observed for the Spectre in Section 5 does not occur here.

### 7.3 The orientation spectrum, and the 2-adic route

Let the 24 proper rotations be the species and let $M_{FF'}$ count the children of an $F$-oriented chair that are $F'$-oriented. The characteristic polynomial is $x^3(x-8)(x-2)^{20}$, the minimal polynomial divides $x(x-8)(x-2)$, every row and column sums to 8, and rank $M^n = 21$ for all

$n \geq 1$. The zero sector is semisimple, there is no negative eigenvalue, and orientation frequencies converge to $1/24$ at the rate $(2/8)^d$ in the depth $d$. The Spectre's matrix is the opposite on each count: a Pisot unit, irrational frequencies and a zero sector with a Jordan pair. The consequence is a narrowing. The Pisot route to pure-point diffraction and the irrational-frequency witness of aperiodicity (Section 2) both need an inflation that is a Pisot number and frequencies that are irrational, and an integer inflation 2 with rational frequencies supplies neither.

The replacement is 2-adic, and it is classical: the undecorated chair substitution, in any dimension, is a standard example of a lattice substitution with a modular coincidence, pure point diffractive with a 2-adic internal space [13, 14]; for the labels of the Chair44 it is recorded in [4, Thm 8.1]. The substitution acts on $24 \times 7 = 168$ labelled unit cells, is primitive (every entry of its $168 \times 168$ matrix is positive at power 3), and has a modular coincidence: at depth 3 there are 336 of 512 addresses, among them $(0, 0, 2)$, at which all 168 labels expand to the same label. By the theorem of Lee and Moody (2001) with Schlottmann (2000) [13, 17, 18], a primitive lattice substitution with a modular coincidence has fixed-point label classes that are regular model sets with a 2-adic internal space, so its diffraction is pure point and the fixed point is limit-periodic. That implication is a cited theorem and is not re-proved, and it concerns the fixed point; that every tiling lies in the substitution hull, which was left open upstream, is Theorem 4 below. What is added here is a recomputation of the finite part from our own generator, which agrees on the depth and the address, and a rate. A subset automaton on the label sets (only 209 are reachable, 41 of them with more than one label) counts the digit words of length $M$ that have not yet fixed the label: $c(M) = 1, 8, 64, 176, 400, 848, 1744, \ldots$, that is $c(M+1) = 2c(M) + 48$ and $c(M) = 28 \cdot 2^M - 48$ from $M = 3$. This holds for every $M$: the vectors $v_M$ of counts per automaton state satisfy $v_5 = 3v_4 - 2v_3$ exactly, so applying the linear transfer map gives $v_{M+2} = 3v_{M+1} - 2v_M$ for all $M \geq 3$, and $c(M)$ obeys the same recurrence. The undetermined fraction is $c(M)/8^M \sim 28 \cdot 4^{-M}$, and the transfer matrix on the non-singleton states has spectral radius exactly 2, so the set of addresses not yet determined, which is where the window boundaries lie, has box dimension $\log_2 2 = 1$ in the internal space $\mathbb{Z}_2^3$ of dimension 3. The two 2's are the same number as the linear inflation and the subdominant orientation eigenvalue, and no link between them is claimed there; Section 8 finds the first-moment sum rule that both obey. The Spectre rests on a Pisot unit and an irrational window; Tsiokos's Chair44 rests on an integer inflation and a 2-adic one.

### 7.4 Every tiling lies in the hull, and the symmetry groups of tilings

The 2-adic route above is stated for the fixed point of the substitution. Tsiokos left two questions open [4]: whether *every* tiling by the Chair44 lies in the hull of the substitution, and which symmetry groups its tilings have. The decorations force every tiling to be hierarchical: a short Berger-style account is due to Goodman-Strauss [5], simpler equivalent matching rules to Flicker [6], and a finite certificate for the unique hierarchy to Kamenetsky [12]. Flicker argues informally that no slide plane is possible and states that only 30 of the 44 contacts appear in an infinite tiling; Theorem 4 and Corollary 1 are the rigorous form. This subsection answers the two questions. The proofs are due to the second author [7]; they combine one level of the hierarchy with a finite computation on the eight unit cells around a lattice vertex.

**Set-up.** A chair *pose* is $x \mapsto gx + t$ with $g$ one of the 24 proper rotations $O$ and $t \in \mathbb{Z}^3$. An *atlas tiling* is a tiling of $\mathbb{R}^3$ by chairs in poses in which every face-adjacent pair has a relative pose among the 44 legal contacts of Section 7. Label each unit cell by the frame of the chair

that covers it and by which of its seven cells it is; there are 168 labels, the $24 \times 7$ of Section 7. Write $\sigma$ for the substitution, of inflation 2.

**Definition 1.** A *block* is the labelling of the eight unit cells around a lattice vertex. It is *legal* if it occurs in $\sigma^n(j)$ for some label $j$ and some $n$, and *admissible* if the chairs it names are consistent and pairwise disjoint and every face-adjacent pair has a relative pose among the 44 legal contacts. Every block of an atlas tiling is admissible.

One input is taken from the literature and is not re-derived here; the other is proved below from a finite certificate that is checked independently.

**(R)** Every tiling by $Q$ is, up to an isometry, an atlas tiling: it is registered, and every pair of tiles sharing a feature is in a relative pose among the legal contacts [4, Thm 5.6, Lemma 5.3]; every shared unit face carries features. This is the geometric half of [4]. Its written proof has been audited step by step by the second author, and all of its finite inputs recomputed in exact arithmetic, including each of the 5,273 collision witnesses (`chair44_independent/registration_audit.py`, `REGISTRATION_AUDIT.md`) [7]; no gap was found. Tsiokos's formal proof of it [4] has also been rebuilt from source in an independent build. The build succeeds, and the dependency report of the theorem lists only the three standard axioms of the proof assistant and named decision steps evaluated by its compiler; the report is identical to the published one (`lean_rebuild/`). It has not been refereed.

**(H)** Every atlas tiling $T$ partitions uniquely into complete level-1 supertiles, which form an atlas tiling $D(T)$ with $T = \sigma(D(T))$. This is Kamenetsky's Proposition 7.1 [12] applied to the Chair44, and Tsiokos proves it for tilings by $Q$ [4, Thms 6.4, 6.5]. It is proved here as Lemma 1.

**Lemma 1** (Kamenetsky's criterion, checked)**.** *(H) holds.*

*Proof.* Call two chairs compatible if their interiors are disjoint and, if they share a unit face, their relative pose is one of the 44 legal contacts. An enclosure of a chair $A$ is a set of pairwise compatible chairs, compatible with $A$, covering its 24 unit faces; it is live if the chairs of $A$ and the enclosure can all have their faces covered again by pairwise compatible chairs. Three finite facts are checked by `hierarchy_certificate/check_chair44_hierarchy.py`, written independently of [12] and [7]. (C1) The relative poses of touching children in the supertiles of all levels are 30. The poses of a level-1 supertile that are admissible next to a reference supertile, with all 64 child pairs compatible, are all aligned; they are exactly the doubles $(g, 2t)$ of the 44 legal contacts $(g, t)$. The coarsening closure of the 30 is therefore the 44, and these 44 are the contacts of the atlas; they are also exactly the poses that obey the 135 face-to-face rules the 44 induce. (C3) A chair has 33 enclosures, 18 of them not live. For each of the 15 live ones exactly one level-1 supertile containing $A$ is compatible with $A$ and the enclosure (U). Either $A$ is that supertile's central child $T_0$ and all eight children are already present, or $T_0$ is a chair of the enclosure and every enclosure of $T_0$ compatible with $A$ and the enclosure contains all eight children (Pr).

Let $T$ be an atlas tiling and $A$ a tile of $T$. Its enclosure $E$ in $T$ is one of the 33, and it is live because the rest of $T$ covers the faces again; so (U) gives a unique supertile $S(A)$ compatible with $A \cup E$. Any supertile of $T$ containing $A$ is compatible with $A \cup E$, so it can only be $S(A)$. By (Pr), applied to the enclosure of $T_0$ in $T$, all eight children of $S(A)$ are tiles of $T$. If $A'$ is another child, $S(A)$ is compatible with $A'$ and its enclosure, all of whose chairs are tiles of $T$,

so $S(A') = S(A)$. The supertiles $S(A)$ therefore partition $T$, and the partition is unique. Two touching supertiles of the partition have all their touching child pairs among the 44 contacts, so by (C1) their relative pose is $(g, 2t)$ with $(g, t)$ legal. Halving gives an atlas tiling $D(T)$ with $T = \sigma(D(T))$. □

**Lemma 2** (computation)**.** *There are 360,189 admissible blocks, in* 15,214 *orbits under $O$. For each of them, all* 27 *windows of size* $2 \times 2 \times 2$ *in its substitution, a* $4 \times 4 \times 4$ *block, are legal.*

A third implementation, written from the definitions for a referee review of this paper and sharing no code with the others, derives the 44 contacts from Tsiokos's pyramid data and reproduces 360,189 admissible blocks, 15,214 orbits and no illegal child window, checking every block and not only orbit representatives (`https://github.com/romanov360/big-bang-monotile`, `research/spectre_review`). It is the second author's computation (`chair44_vertex_blocks.py` and `chair44_hull_prune.py`, on the atlas published with [4]), repeated by an independent implementation that derives the atlas from the pyramid geometry and, separately, from the eight children alone, and published as a certificate of $O$-orbit representatives with a stand-alone verifier [7]. `chair44_hull_admissible.py` repeats the count with the 44 contacts that `symchair44.py` derives from its own labels; this is independent code on the same eight children, which define the tile. The lemma is not vacuous: enlarging the atlas by the five non-atlas contacts of a single violating block yields 360,213 admissible blocks and 24 failures. The count runs for minutes, so the build of this paper does not repeat it.

**Theorem 4.** *Every atlas tiling lies in the hull $\Omega_\sigma$ of the substitution. Hence, by (R), every tiling by $Q$ lies, up to an isometry, in $\Omega_\sigma$.*

*Proof.* Let $P$ be a finite patch of an atlas tiling $T$. By (H) every $D^m(T)$ is an atlas tiling on a lattice $L_m = 2^m\mathbb{Z}^3 + o_m$, $L_{m+1} \subset L_m$. For $2^{n-1}$ larger than the diameter of $P$, $P$ lies in $\sigma^n(\beta)$ for the block $\beta$ of $D^n(T)$ at the vertex $v$ of $L_n$ nearest to $P$, and $\beta$ is the window at offset $v - v' + (1, 1, 1)$ of $\sigma(\beta')$ for the block $\beta'$ of $D^{n+1}(T)$ at the vertex $v'$ of $L_{n+1}$ nearest to $v$. As $\beta'$ is admissible, $\beta$ is legal by Lemma 2, and so is $P$. No exhaustion of space by one supertile is used, so tilings with fault planes are covered. □

**Corollary 1.** *Only the* 30 *contacts that occur in supertiles appear in an atlas tiling; the other* 14 *legal contacts occur in none.*

*Proof.* The block at a corner of a shared unit face contains both cells across it, and the face-adjacent pairs in legal blocks realise exactly the 30 supertile contacts. □

**Corollary 2.** *$\Omega_\sigma$, under translations of $\mathbb{R}^3$, is minimal and uniquely ergodic with pure-point dynamical spectrum, and it is the hull of a regular model set with internal space $\mathbb{Z}_2^3$. Every atlas tiling is pure-point diffractive; by (R), so is every tiling by $Q$.*

*Proof.* The substitution is primitive, so $\Omega_\sigma$ is minimal and uniquely ergodic. The modular coincidence of [4, Thm 8.1], recomputed above, and the theorem of Lee and Moody [13] give pure-point spectrum of the hull [18]. In a uniquely ergodic hull every element has the same diffraction, and Theorem 4 places every atlas tiling in $\Omega_\sigma$. □

The space of all tilings by $Q$ is not minimal: it is the union of the translates $g\Omega_\sigma$ over the isometries $g$. Nor is every element of $\Omega_\sigma$ a model set or limit-periodic; singular elements of a model-set hull need not be.

**A second route to the finite part.** The legal blocks depend only on the substitution, so they can be recomputed from the cell substitution of Section 7, which our generator builds from nothing (`chair44_hull.py`). The distinct $2\times2\times2$ windows of $\sigma^n(j)$ over all 168 labels number 168, 600, 1278, 1398, 1410, 1410 for $n=1,\dots,6$, so 1410 blocks are legal. The set is closed, in that all 27 child windows of every one of its members lie in it, and it contains the windows of $\sigma(j)$; so it is the whole language and not merely the place where a count stopped. The central window $\Phi(w)$ of $\sigma(w)$ maps the legal blocks to themselves and has exactly 27 periodic blocks, all of them fixed. These are the 27 fixed seeds of [4], and their stabilisers in $O$ have order 1 for 24 of them and 8 for 3. Both counts agree with the second author's.

**Symmetry.** Write $\mathrm{Sym}(T)$ for the group of isometries that map an atlas tiling $T$ to itself, chairs with their frames; for a tiling by $Q$ this is its geometric symmetry group, since $Q$ has no self-isometry (Fact 18). A symmetry maps poses to poses, so its linear part is a quotient of two proper frames: it is proper, with integer translation part, and its kernel consists of periods, which vanish by (H). So $\mathrm{Sym}(T)$ embeds in $O$, as Tsiokos showed for tilings by $Q$, with $|\mathrm{Sym}(T)|\le 24$; he exhibited orders 1 and 8 [4].

**Theorem 5.** *For every atlas tiling $T$, $\mathrm{Sym}(T)$ is conjugate in $O$ to exactly one of $1$, $C_2^{\mathrm{diag}}$ (a half-turn about a face-diagonal axis), $C_4$ and $D_4$, and each occurs. By (R), the same holds for every tiling by $Q$.*

**Lemma 3** (position of symmetry axes)**.** *Let $L_n=2^n\mathbb{Z}^3+o_n$ be the vertex lattice of the level-$n$ supertiles of an atlas tiling $T$, so that $o_{n+1}\equiv o_n \pmod{2^n}$, and let $g\in\mathrm{Sym}(T)$ have linear part $R\neq I$. (1) If $R$ is a half-turn or quarter-turn about a coordinate axis, the axis of $g$ is a lattice line of every $L_n$. (2) If $R$ is a half-turn about a face diagonal, the axis of $g$ lies in a coordinate plane through vertices of every $L_n$ and meets every $L_n$. (3) If $\mathrm{Sym}(T)$ is not cyclic, its fixed point is a vertex of every $L_n$. In cases (1) and (2) no single point of the axis need be a vertex of every $L_n$.*

*Proof.* The hierarchy is unique by (H), so $g$ preserves every $L_n$. Write $g(x)=R(x-c)+c$ with $c$ on the axis; since $R$ preserves $2^n\mathbb{Z}^3$, $g$ preserves $L_n$ if and only if $(I-R)(c-o_n)\in 2^n\mathbb{Z}^3$. (1) Take the axis along $e_3$. For a half-turn $I-R=\mathrm{diag}(2,2,0)$; for a quarter-turn $I-R$ acts on the $(e_1,e_2)$-plane with determinant 2. Either way each $\delta_n^{(i)}=(c_i-o_{n,i}) \bmod 2^n$, $i=1,2$, is 0 or $2^{n-1}$ (for $n=0$: 0 or $\frac12$). If $\delta_n^{(i)}=2^{n-1}$ then, since $o_{n+1}\equiv o_n \pmod{2^n}$, $c_i-o_{n+1,i}\equiv 2^{n-1}$ or $3\cdot2^{n-1} \pmod{2^{n+1}}$, neither 0 nor $2^n$, against the condition at level $n+1$. So every $\delta_n^{(i)}=0$. (2) For $R(x,y,z)=(y,x,-z)$ the condition reads $(c_1-o_{n,1})-(c_2-o_{n,2})\in 2^n\mathbb{Z}$ and $2(c_3-o_{n,3})\in 2^n\mathbb{Z}$. The second gives $c_3\equiv o_{n,3}$ as in (1); by the first, $c+s(1,1,0)$ lies in $L_n$ for $s\equiv o_{n,1}-c_1$. (3) A non-cyclic subgroup of $D_4$ contains two half-turns about perpendicular coordinate axes, or one about a coordinate axis and one about a perpendicular face diagonal; its fixed point is the intersection of the two axes, and by (1) and (2) each of its coordinates is $\equiv o_n \pmod{2^n}$. □

*Proof of Theorem 5. No element of order three.* Such an element is a rotation about a line in direction $(1,\pm1,\pm1)$. Along the line the three coordinates change at the same rate, so at some point all three lie in $(\frac{1}{100},\frac{99}{100})$ modulo 1. That point is interior to a unit cell, hence to the chair covering it (for $Q$: farther from every cell face than the pyramid height $12\cdot10^{-4}$), so the rotation fixes that chair with its frame and is the identity. So $\mathrm{Sym}(T)$ is a 2-group, contained in a copy of $D_4$; up to conjugacy in $O$ its candidates are 1, $C_2$ (coordinate axis), $C_2^{\mathrm{diag}}$, $C_4$, the two Klein groups and $D_4$. By Theorem 4 every block below is legal.

*Vertex-centred groups.* Let $\mathrm{Sym}(T)$ be non-cyclic, with fixed point $x$, a vertex of every $L_n$ by Lemma 3(3), and let $w_n$ be the block of $D^n(T)$ at $x$. Then $w_n = \Phi(w_{n+1})$. The substitution commutes with $O$, so $\mathrm{Stab}(w_{n+1}) \le \mathrm{Stab}(w_n)$, and since the $w_n$ cover balls of radius $2^n$ about $x$, $\mathrm{Sym}(T) = \bigcap_n \mathrm{Stab}(w_n)$; the stabilisers are constant from some $N_0$ on. A block $\beta$ that occurs infinitely often among $w_{N_0}, w_{N_0+1}, \dots$ satisfies $\beta = w_a = w_b$ with $N_0 \le a < b$, so it is $\Phi$-periodic and $\mathrm{Stab}(\beta) = \mathrm{Sym}(T)$. The $\Phi$-periodic legal blocks are the 27 fixed seeds, with stabilisers 1 and $D_4$; this is the count recomputed above. So a non-cyclic group is $D_4$, and the Klein groups do not occur.

*Axial groups.* Let $\mathrm{Sym}(T) = K$ be cyclic and non-trivial, with axis $A$ in direction $e$, and let $O_e$ be the rotations about $e$. By Lemma 3, $A \cap L_n = v_n + 2^n\mathbb{Z}e$; take $v_n$ nearest to a fixed point $p$ of $A$. Then $v_n - v_{n+1} = j_n 2^n e$ with $j_n \in \{-1, 0, 1\}$, and the blocks $w_n$ of $D^n(T)$ at $v_n$ satisfy $w_n = W_{j_n}(w_{n+1})$, where $W_j$ is the window of $\sigma(\cdot)$ centred at $je$. The elements of $O_e$ commute with every $W_j$, so $\mathrm{Stab}(w_n) \cap O_e$ decreases to $K$; the full stabilisers may be larger, since an element outside $O_e$ acts about the moving point $v_n$. If $j_n = j$ for all $n \ge N$, then $y = v_N + j2^N e$ satisfies $y - v_n = j2^n e$ for $n \ge N$, so $y$ is a vertex of every $L_n$ and $\mathrm{Sym}(T)$ is 1 or $D_4$ by the previous case, not $K$. So the shifts are not eventually constant, and their tail lies in a strongly connected component carrying two distinct shifts of the graph $G_K$ whose vertices are the legal blocks $w$ with $\mathrm{Stab}(w) \cap O_e = K$ and whose edges $w \to W_j(w)$ are labelled $j$.

Conversely, take a cycle in $G_K$ whose labels $j_0, \dots, j_{p-1}$ are not all equal and unroll it periodically: $v_n = p - x_n e$ with $x_n = \sum_{m<n} j_m 2^m$. With $J_i = \sum_{m<p} j_{i+m} 2^m$ (indices mod $p$) and $y_i = J_i/(1-2^p)$, induction gives $x_n = y_0 - 2^n y_{n \bmod p}$; since $0 < |J_i| < 2^p - 1$, $|x_n| \le \mu 2^n + 1$ with $\mu = \max_i |J_i|/(2^p - 1) < 1$, so the blocks cover cubes of half-width $(1-\mu)2^n - 1$ about $p$ and define a tiling in the hull. Every element of $K$ fixes $A$ and stabilises every $w_n$ about $v_n \in A$, so $K \le \mathrm{Sym}(T)$. A point $p + ze$ lies in every $L_n$ only if $z$ is the 2-adic number $-y_0$, which is not an integer; by Lemma 3(3) the symmetry group is cyclic about $A$, hence $K$.

A computation finds such components for $C_2^{\mathrm{diag}}$ (14 blocks on each face-diagonal axis) and $C_4$ (4 blocks). For a half-turn about a coordinate axis the 18 blocks of $G_K$, among them blocks whose full stabiliser is $D_4$ or a Klein group, form only components of constant shift. Explicit tilings built from such cycles show exactly the predicted group on large central regions; that is a consistency check, and the exclusion of further symmetries rests on the argument above. □

*Remark* 1. In particular $|\mathrm{Sym}(T)| \le 8$, and the bound is attained. No atlas tiling has a 3-fold axis, a Klein four-group of symmetries, or exactly a 2-fold coordinate axis.

The theorem is about tilings and does not conflict with Fact 18, which is about the tile: the decorated chair has only the identity, and a tiling by it can still be invariant under a rotation of its whole pattern. Nor does the bound of 8 conflict with the 24 orientations that occur in a depth-three supertile (Fact 19): by Theorem 4 every tiling contains all of them, and it is symmetric under at most a third of the 24 rotations.

**Scope.** For atlas tilings, Theorem 4, Corollaries 1 and 2 and Theorem 5 rest on Lemma 1, on Lemma 2, and, for the corollary, on the theorem of Lee, Moody and Solomyak. For tilings by $Q$ they also rest on (R), quoted, audited by the second author, and not refereed. The admissible-block count, the axial-group analysis and the explicit patches are the second author's computations, repeated independently; the build of this paper recomputes the language of legal blocks, its closure, the fixed seeds and their stabilisers. None of this bears on the einstein property or on strong aperiodicity of the Chair44, which remain Tsiokos's claim.

### 7.5 Uniform frequencies hold in boxes, not along lines

Corollary 2 says that every finite patch has a frequency, reached uniformly by boxes of side $L$ in every tiling. It is tempting to read this as a statement about any scan of a tiling, for instance the sum of an observable along a line of cells. It is not, and this subsection says what is true. Everything below is an exact finite computation (`chair44_lines.py`) except the last proposition, which is conditional on the internal space of Corollary 2.

**Box means.** The matrix of the cell substitution on the 168 labels is primitive with every row and column sum 8, so each label has frequency $1/168$ in every tiling, and the box mean of a cell observable is its mean over the labels. We use two observables of a cell. The *height* $p$ is the sum of the signed heights of the pyramids on the faces of the cell; it vanishes on five of the seven cells of the chair and is $-36$ and $+36$ on the other two (the two values cancel, as they must, since the 192 heights sum to zero). The *notch vector* $d = g(1,1,1) \in \{\pm 1\}^3$ belongs to the chair that covers the cell. Both have box mean exactly 0, in each component.

**Proposition 3** (chair stacks)**.** *Six of the 168 labels, namely cell* 0 *of the chairs whose notch points along* $\pm(1,1,1)$ *(three along each sign), satisfy* $\sigma(j)_{000} = \sigma(j)_{111} = j$*. For each of them and every* $n$*, the chairs of* $\sigma^n(j)$ *form a stack in which each chair fills the notch of the next, and each of the seven cells of the chair gives a line of identical labels, of length* $2^n - 2$*, in direction* $(1,1,1)$*. Along such a line* $p$ *is constant,* $-36$ *on one cell type and* $+36$ *on another, and each component of* $d$ *is* $\pm 1$*.*

*Proof.* Label the cells $(x, y, z)$ of the stack by the difference $e = (x - z, y - z)$. The lines of the stack are exactly the cells whose difference lies in a set $T$ of seven values, and a cell of difference $e$ has a label $\Lambda(e)$. We show that every cell of $\sigma^n(j)$ with difference in $T$ has the label $\Lambda(e)$, by induction on $n$. For $n = 0$ the single cell has difference $(0,0)$ and label $j = \Lambda(0,0)$. A cell of $\sigma^{n+1}(j)$ is the child $(a,b,c) \in \{0,1\}^3$ of a cell of $\sigma^n(j)$ whose difference is $e' = \big((e_0 - a + c)/2, (e_1 - b + c)/2\big)$. So it suffices that, for every $e \in T$ and every child position compatible with $e$, the difference $e'$ lies in $T$ and $\sigma[\Lambda(e'), (a,b,c)] = \Lambda(e)$. That is 14 cases for each of the six labels, and they all hold (`chair44_lines.py`). The main diagonal is the case $e = (0,0)$. □

The stack lies in every tiling. It occurs in $\sigma^n(j)$ for every $n$, and by Theorem 4 and minimality every legal patch occurs in every tiling. So in every Chair44 tiling and for every $L$ there are $L$ consecutive cells on a line in direction $(1,1,1)$ on which the mean of $p$ is exactly $-36$ (and others on which it is $+36$) and the mean of each component of $d$ is $\pm 1$, while the box means are 0. Averages along these lines do not converge to the box mean, and no uniformity in $L$ can hold for them.

**Corner lines.** For $b \in \{0,1\}^3$ the cells $tb$ of $\sigma^n(j)$, $0 \le t < 2^n$, are the $n$-th iterate of the constant-length-2 substitution $\tau_b(j) = \sigma[j,0]\,\sigma[j,b]$ on the same labels, since the child positions along the line are always 0 and $b$. Its closed strongly connected classes, each primitive and each reached from every label, carry exact letter frequencies and so exact limits of the mean of each cell observable along the line, for each starting label. Table 4 gives the mean of the notch vector; the mean of $p$ is 0 on all of them. The seven lines are the lines through the corner of the cube in the seven directions in $\{0,1\}^3$; they are also read off the label cube, with agreement.

Table 4: Corner lines of $\sigma^n(j)$: closed classes of $\tau_b$ and the exact limit of the mean of the notch vector. The box mean is $(0,0,0)$.

| direction $b$ | closed classes of $\tau_b$ | mean of $d$ |
|---|---|---|
| $(0,0,1)$ | one class of 4 | $(1,1,0)$ |
| $(0,1,0)$ | one class of 4 | $(1,0,1)$ |
| $(0,1,1)$ | one class of 4 | $(1,0,0)$ |
| $(1,0,0)$ | one class of 4 | $(0,1,1)$ |
| $(1,0,1)$ | one class of 4 | $(0,1,0)$ |
| $(1,1,0)$ | one class of 4 | $(0,0,1)$ |
| $(1,1,1)$ | 6 fixed letters | $(-1,-1,-1)$ and $(1,1,1)$ |

**Proposition 4.** *Assume that the hull $\Omega$ of label configurations, under the action of $\mathbb{Z}^3$ by translations, has maximal equicontinuous factor $\pi : \Omega \to \mathbb{Z}_2^3$ with $\pi_*\nu$ the Haar measure (Corollary 2; for the action of $\mathbb{R}^3$ on tilings the factor is a solenoid, not $\mathbb{Z}_2^3$). Let $v \in \mathbb{Z}^3 \setminus 0$. Then the action of the translation $T^v$ on $\Omega$ is not uniquely ergodic. There are a function $f$ of a finite window of labels and a tiling $T$ such that the averages $\frac{1}{L}\sum_{t<L} f(T^{tv}T)$ along the line through 0 in direction $v$ converge to a number different from $\int f\, d\nu$.*

*Proof.* The closure of $\{tv : t \in \mathbb{Z}\}$ in $\mathbb{Z}_2^3$ is $H = \mathbb{Z}_2 v$, a closed subgroup of infinite index, so its Haar measure is 0. For $x \in \Omega$ the set $K = \pi^{-1}(\pi(x) + H)$ is compact, non-empty and $T^v$-invariant, so it carries a $T^v$-ergodic probability measure $\mu$. Since $\nu(K) = 0$, $\mu \neq \nu$, and functions of a finite window of labels are dense in $C(\Omega)$, so some such $f$ has $\int f\, d\mu \neq \int f\, d\nu$. By Birkhoff's theorem the averages along the line converge to $\int f\, d\mu$ for $\mu$-almost every tiling. □

Proposition 3 and Table 4 are explicit instances for the directions $(1,1,1)$ and the others in $\{0,1\}^3$. The failure depends on the observable and on the line: the corner lines all have $p$-mean 0, and a coordinate-axis line can have bounded sums of $d_z$ while another has sums of $d_z$ growing like $L$. Nothing here concerns directions that are not lattice directions: the cells met by a line of irrational slope are not an orbit of a subgroup of $\mathbb{Z}^3$, and the argument does not apply.

### 7.6 Why Three Dimensions Do Not Automatically Resolve Chirality

A common heuristic about parity rests on a sentence: a planar patch embedded in a three-dimensional bulk has its reflection realized as an ambient rotation, so parity that is forbidden on the surface is restored by embedding. The Chair44 does not touch that sentence. It does touch the suggestion that three dimensions are what restores parity.

**Fact 18.** *The undecorated seven-cube chair has* 6 *symmetries, 3 of them mirrors, and is achiral. The decorated Chair44 has only the identity, so it is chiral. Of the* 2388 *raw face contacts,* 1194 *place a mirror image against the root, and none is legal: all* 44 *legal contacts are proper rotations, so no copy of the tile touches its own mirror image anywhere in the hierarchy.*

The chirality is forced twice over: by the labels, which break the three mirror planes of the seed, and by the contacts, which admit no mirror pair. So, for this tile, passing from the plane to three dimensions does not by itself make mirror images available. Three caveats attach. The einstein property is Tsiokos's claim. The forced chirality was tested on all six substitutions that leave twelve height classes and does not depend on the selection rule, but a decoration outside

that family is not excluded. And one example is one example: a three-dimensional aperiodic tile whose legal contacts include a mirror image would show that forced chirality is not a feature of dimension three (`symchair44.legal_contacts` tests any labelled candidate). This section does not show that the Chair44 is an einstein monotile, or aperiodic, or that the pyramid decoration is the only one that works; it re-derives its atlas and finds it equal to the published one. A numerical scan of sliding and tilted placements of smoothed variants (`chair44_rigidity.py`) found no non-lattice contact, which is evidence for rigidity and not a proof of it.

# 8 Unfolding the Chair44 and Comparing it with the Spectre

Section 7 compared the two tilings by their combinatorics. This section brings the three-dimensional tile down to two dimensions in the two exact ways, unfolding its surface into a net and slicing and projecting the hierarchy, and then asks the same questions of both tilings. Each tile is reduced to a point (the centroid of a Spectre, the centre of the bounding cube of a chair) and an orientation vector ($e^{i\theta}$ for a Spectre, the direction $d = g(1,1,1)$ of the missing corner, the notch, for a chair). Every number is a Fact computed by `chair44_unfold.py`, `chair44_slice.py` and `chair44_findings.py`, with the Spectre sums on the patches of `spectre.py` through level 5, which has 34649 tiles.

## 8.1 The twist of the Tsiokos Chair44 supertile

Fact 6 computed the twist of the Spectre supertile. The same question for the Chair44 has a simpler answer.

**Fact 19.** *The eight chairs of the supertile fill the doubled chair cell for cell, so the inflation is a scaling by* 2 *with no rotation and no mirror: its twist is* 0*. The eight child frames are proper rotations through* $0, 90, 120, 180$ *degrees, two of each, and their mean matrix is exactly* $I/4$*, so the mean frame over the* $8^n$ *chairs of a level-n supertile is* $I/4^n$*. All* 24 *rotations of the cube occur already at depth two.*

The Spectre supertile is turned by $\theta_S = 11.565°$ and mirrored at every level (Fact 6), and $\theta_S$ is irrational as an angle; every child rotation of the chair is a rational multiple of $\pi$, so no irrational twist can arise from this substitution. The mean matrix $I/4$ is the statement $\sum_i H_i = 2I$: the eight child rotations add up to the linear inflation times the identity. This is a first-moment sum rule, and it is the only structure found here that links the two 2's noted at the end of Section 7; whether it is related to the repeated eigenvalue 2 of the orientation matrix is not shown.

## 8.2 Polyhedral Unfolding and Surface Net Construction

The surface of the chair is a sphere made of 24 unit squares, with 26 vertices and 48 edges, whose folds are 27 convex, 18 flat and 3 concave. Cutting it along a spanning tree of its face-adjacency graph, 23 cuts, and folding every face into the plane gives a 24-omino. There are 261,434,325,600 spanning trees (the matrix-tree theorem, exact). Of 3000 random trees, 1253 give a valid net and 1747 overlap themselves; the valid nets have perimeters from 28 to 50, and 2 of them tile the plane by translation. The smallest perimeter found is a sampled value and not a minimum (any 24-omino has perimeter at least 20). The control is the same code on a single cube, over all 384 of its spanning trees: it returns exactly the 11 nets of the cube. Figure 4 shows three nets and the perimeters.

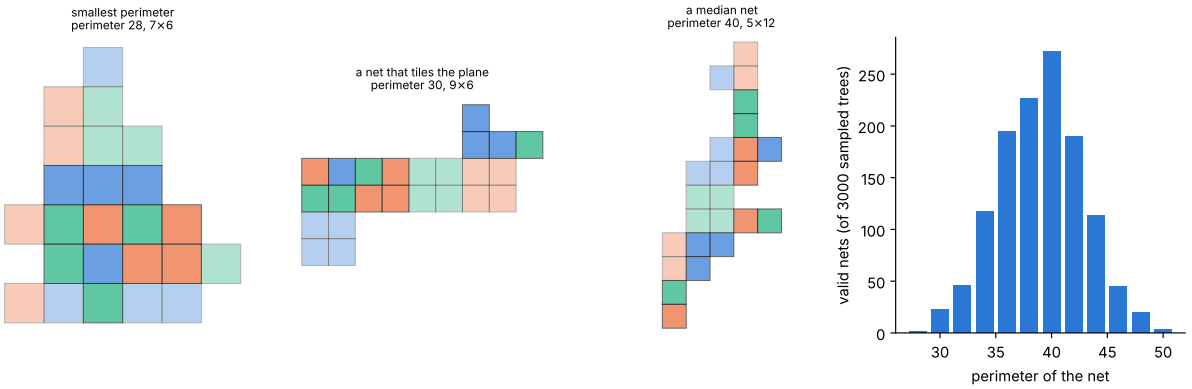


Figure 4: Unfolding the surface of the chair. Three nets (colour is the axis of the face normal, strong for the outward + side): the smallest perimeter among the sampled valid nets, one of the nets that tile the plane by translation, and a median one; and the perimeters of all the valid nets in the sample.

The supertile surface is the chair surface scaled by 2, so its net is the chair net with each square replaced by a $2 \times 2$ block: the area grows by 4 and the length by 2, which is the dimension $D_b = 2$ already found for the boundary (Section 7). Unfolding therefore does not produce a planar analogue of the Spectre's outline, whose perimeter grows with exponent 1.3993 at every order. That is a negative result, and the exact boundary count had already implied it.

### 8.3 Chair44: Slices, projections and the notch vector

A layer $z = c$ of the depth-$n$ patch cuts each chair it meets into a square of 4 cells or an L-tromino of 3 (the cross-sections found are 3 and 4 cells), so a slice is a tiling of a planar region by polyominoes. The projection of the chair centres along $z$ has, by the projection theorem, the $k_z = 0$ plane of the three-dimensional diffraction as its Fourier transform; this was checked against a three-dimensional FFT.

**Fact 20.** *The $8^n$ centres of the bounding cubes of the depth-$n$ patch are distinct integer points on two cosets of $2\mathbb{Z}^3$ ($7, 56, 448, 3584$ and $1, 8, 64, 512$ points for $n = 1, \ldots, 4$), and the notch vectors sum to $2^n(1, 1, 1)$. The interface length inside the layer $z = 0$ is $4^{n+1} - 4 \cdot 2^n$ for $n \leq 4$ ($8, 48, 224, 960$).*

The sum of the notch vectors in Fact 20 is the sum rule of Fact 19 applied to the vector $(1, 1, 1)$, and it was also counted. It is far smaller than the sum of $8^n$ random signs, which is of order $8^{n/2}$: the intensity of the notch-weighted structure factor at the origin per tile is $3 \cdot 2^{-n}$ instead of order 1. The layer interface grows by a factor tending to 4 per level, again dimension 2. Figure 5 shows a slice, the $k_z = 0$ plane at level 5, the origin values, and the median intensity at random wave vectors.

### 8.4 The same questions asked of the Spectre

The orientation sum of the Chair44 grows by exactly the linear inflation, 2 per level. The same sum for the Spectre can be computed on the placed tiles.

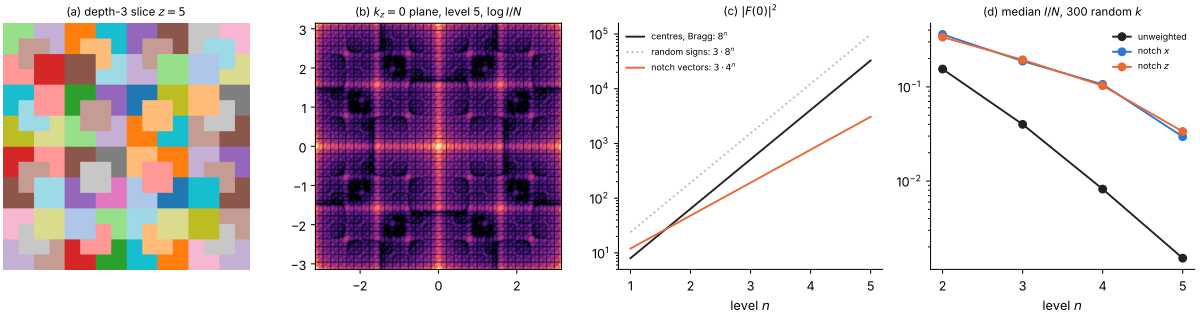


Figure 5: Slices and projection of the hierarchy. (a) A depth-3 layer, coloured by tile. (b) The $k_z = 0$ plane of the diffraction of the level-5 chair centres, which is the Fourier transform of their projection. (c) The squared structure factor at the origin: the centres (Bragg, $8^n$), random signs ($3 \cdot 8^n$) and the notch vectors ($3 \cdot 4^n$). (d) The median of $I/N$ at 300 random wave vectors, unweighted and weighted by a notch component.

**Fact 21.** *For the Chair44 the notch sum is* $2^n$ *exactly* $(4, 8, 16, 32$ *at levels* $2, \dots, 5)$*. For the Spectre,* $|\sum_j e^{i\theta_j}|/\lambda^n = 1.4413, 1.4480, 1.4488, 1.4489$ *at levels* $2, \dots, 5$ *(patches of* $71, 559, 4401, 34649$ *tiles), and the ratio of the last two sums is* $2.8061$ *against* $\lambda = 2.8059$*. The first is exact and the second is a measurement over floating-point sums, with no proof.*

In both tilings the orientation sum grows like the linear inflation. The tile counts grow like $\lambda^{dn}$, so $|S|^2/N \propto \lambda^{(2-d)n}$ is constant for the Spectre ($d = 2$; the values are $1.8136, 1.8303, 1.8324, 1.8327$) and $2^{-n}$ for the Chair44 ($d = 3$). On this evidence the two tilings differ in that quantity through the dimension alone, and not through the details of the tile. This is an observation about one choice of orientation weight; it is not a theorem for the Spectre, whose inflation reverses orientation, so that a sum rule of the form $\sum H_i = \lambda I$ is not available to it in the same way.

Where the power goes is asked with a deliberately loose statistic: the median of $I(k)/N$ over 300 fixed random wave vectors, with $k$ in the box $[0, 2\pi/\ell]^d$, against the number of tiles. It falls in both, as $N^{-0.34}$ for the Spectre centroids and $N^{-0.72}$ for the Chair44 centres, and as $N^{-0.26}$ and $N^{-0.39}$ with orientation weights: the intensity is concentrated on few wave vectors, as in a Bragg spectrum, and faster for the chair, whose centres lie on a lattice with defects. Figure 6 and Table 5 gather the comparison.

Table 5: The two tilings under the same questions (Facts 19 and 21). The first four rows are exact; the sum and the slopes of the Spectre are measurements on placed patches.

| | Spectre | Chair44 |
|---|---|---|
| supertile twist | $11.565°$, mirrored each level | 0, no mirror |
| orientations | 12 (steps of $30°$) | 24 rotations |
| supertile outline, dimension | 1.3993 | 2 |
| tile count per level | $\lambda^2 \approx 7.87$ | 8 |
| orientation sum | $\approx 1.4489\,\lambda^n$ | $2^n$ exactly |
| $\lvert S\rvert^2/N$ | constant, $\approx 1.83$ | $2^{-n}$ |
| median $I/N$, slope in $N$ | $-0.34$ (weighted $-0.26$) | $-0.72$ (weighted $-0.39$) |

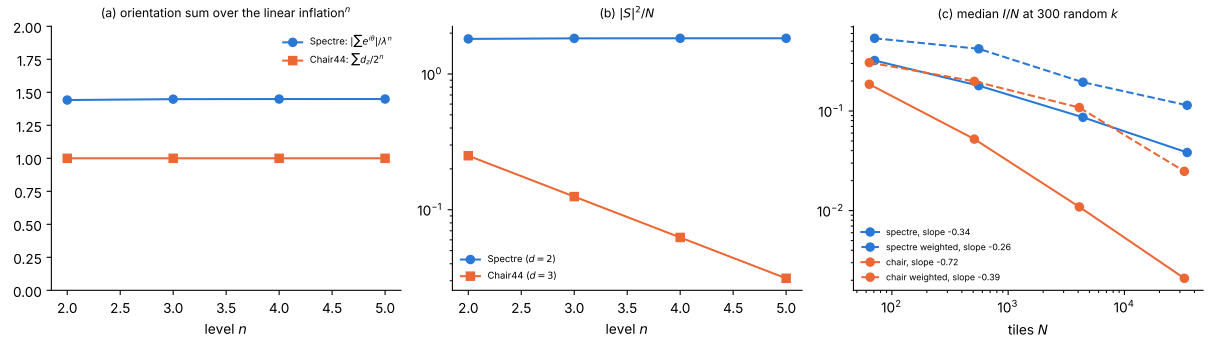


Figure 6: The same questions for both tilings. (a) The orientation sum over the linear inflation to the $n$: constant for both. (b) $|S|^2/N$, the intensity at the origin per tile of the orientation weights: constant for the Spectre, $2^{-n}$ for the chair. (c) The median of $I(k)/N$ at 300 random wave vectors against the number of tiles, unweighted and weighted.

### 8.5 Scope, Limitations, and Epistemic Scope

The nets are a sample of a space of 261,434,325,600 trees, and nothing is claimed about the best net. The point and the orientation vector of each tile are choices, and the sum rule is a statement about the notch vector, not about every function of the orientation. The Spectre patches of `spectre.py` are mirror-type placements; the sum is unchanged by the mirror, but the fixed random wave vectors are not. The median statistic compares two dimensions at one scaling of $k$ and is noisy. None of this decides whether the diffraction measure of either tiling is pure point: for the Spectre that is a published theorem [8, 9], and the exact analysis of the Chair44 centre set is in Section 9.

## 9 Scattering Diffraction, Orientations, and Adjacency Relations

This section asks four exact questions of both tilings. The tools are in the repository of curved-tile programs spectre-monotile-py; each Fact is computed there and in `monotilefacts.py`.

### 9.1 The diffraction of the Chair44 centres

Take one point per chair, the centre of its bounding cube, and call the set at depth $n$ $X_n \subset \mathbb{Z}^3$.

**Fact 22** (Exact diffraction of the centre set)**.** *$X_n = 2X_{n-1} \cup (B_n \setminus B'_n)$, where $B_n$ is the set of odd points of the cube $[1, 2^{n+1} - 1]^3$ and $B'_n$ the odd points with every coordinate above $2^n$ (the corner octant); the recursion reproduces the placed patch for $n \le 4$. The structure factor is a finite sum of products of geometric series and equals the direct sum over the centres (relative difference $1.1e-15$). At the dyadic wave vectors $k = 2\pi m/2^J$, $m$ not all even, its limit is the exact amplitude*

$$a(k) = \tfrac{7}{8}\, 8^{1-J}\big(\pm 1 + \tfrac{1}{7}\big),$$

*with sign $-$ when $m_1 + m_2 + m_3$ is odd, so at $J = 1$, $a = -\frac{3}{4}$ on an axis, $a = -\frac{3}{4}$ on the body diagonal and $a = 1$ on a face diagonal; the last says only that every centre has $x + y$ and $y + z$*

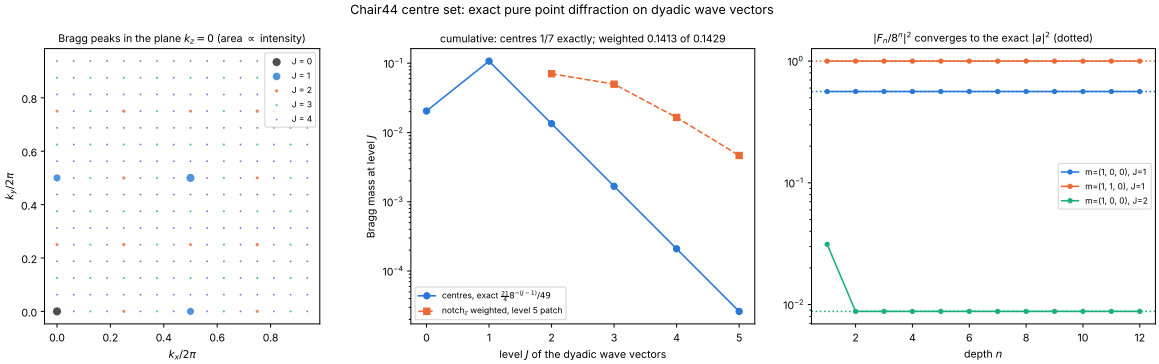


Figure 7: Bragg structure of the Chair44 centre set. The exact amplitudes at the dyadic wave vectors by level, the level masses $\frac{21}{4}8^{1-J}$ and their running sum approaching the density, and the finite-patch intensity converging to it.

*even. The squared amplitudes at level $J$ sum to $\frac{21}{4}8^{1-J}$, and*

$$\frac{1}{49}\Big(1+\sum_{J\geq 1}\tfrac{21}{4}8^{1-J}\Big)=\frac{1}{7}=\textit{density of the centres.}$$

*Wave vectors that are not dyadic carry no amplitude.*

The Parseval sum is complete: all the mass of the density is in the Bragg peaks, so the diffraction measure of the centre set is pure point, and the 2-adic route of Section 7 is made explicit for this set. The centre set depends only on the undecorated chair substitution, so its pure-point diffraction also follows from [13, 14]; what is added is an explicit worked example. The mass of the notch-weighted measure is only numerically consistent with this. That the diffraction of the Spectre is pure point is a published theorem [8, 9] and is not re-proved here; the contrast is only in the route, a cut-and-project scheme with an internal space for the Spectre and a dyadic Parseval sum for the chair.

## 9.2 Orientation sums and their channels

Section 8 measured the sum of the orientation vectors of both tilings. The chair's is exactly $2^n$. For the Spectre it can now be written as a recursion.

**Fact 23** (The orientation recursion)**.** *Let $S_n$ be the vector over the nine tile labels of the sums of $e^{i\theta}$ over the tiles of the depth-$n$ supertile of each label. Then $S_{n+1} = C\,\overline{S_n}$ with $C$ the $9\times 9$ matrix of the slot rotations of the construction; the conjugate appears because the inflation reverses orientation. Two levels give $C\overline{C}$ with leading eigenvalue $\lambda^2 = \sqrt{15}+4$, and the sums over the placed tiles agree with the recursion (largest relative difference $2e-15$, to level 5). Hence $|S_n| \sim c\,\lambda^n$ for a constant $c>0$.*

Numerically, from the recursion to eighty digits, $c^2$ is the root of $400x^4-1200x^3+840x^2-180x+9$ equal to

$$c^2=\frac{15+5\sqrt{3}+3\sqrt{5}+3\sqrt{15}}{20}=2.0994,$$

a closed form that is identified, not proved; it is not part of the Fact. It could be proved exactly from the dominant eigenvector of $C\overline{C}$ over $\mathbb{Q}(\sqrt{3}, \sqrt{5}, i)$.
The constant is the ratio 1.4489 measured in Section 8. Splitting the orientation sums by the irreducible representations of the rotation group of the cube for the chair, and by the harmonic $m$ of the orientation angle for the Spectre, gives the growth exponent of each channel.

**Fact 24** (Orientation channels)**.** *The* 24*-dimensional orientation matrix of the Chair44 has characteristic polynomial* $x^3(x-8)(x-2)^{20}$*: the trivial channel has eigenvalue* 8 *and every non-trivial channel is exactly* 2 *times a projector. With the exponent* $h = \ln \mu / \ln \lambda_{\mathrm{lin}}$ *of the leading eigenvalue* $\mu$ *in the linear inflation* $\lambda_{\mathrm{lin}}$*, the trivial channel has* $h = 3$ *and all others* $h = 1$*. For the Spectre the harmonics* $m \in \mathbb{Z}/12$ *give* $h = 2$ *for* $m = 0, 6$*,* $h = 1$ *for* $m = \pm 1$ *and* $m = \pm 5$ *(the Galois partners of* $\pm 1$ *under* $z \mapsto z^5$*), and* $h \leq 0$ *for* $m = \pm 2, \pm 3, \pm 4$*.*

The intensity at the origin per tile of a channel with exponent $h$ in dimension $d$ scales as $\lambda_{\mathrm{lin}}^{(2h-d)n}$. The chair's orientation weights therefore have $|S|^2/N \propto 2^{-n}$ in the non-trivial channels ($h = 1$, $d = 3$) and the Spectre's has an exponent 0 for $m = \pm 1$ ($h = 1$, $d = 2$), which is the difference drawn in Figure 6.

### 9.3 Which faces meet which

**Fact 25** (Contact matrices)**.** *Count how often native edge* $a$ *of one tile meets native edge* $b$ *of a neighbour. For the Spectre (level-*4 *patch,* 29,208 *contacts) the* $14 \times 14$ *symmetric matrix has* 62 *nonzero entries, rank* 14*, is bipartite, connected, and has a spectrum symmetric about zero. For the Chair44 (depth-*3 *patch,* 5,376 *contacts, equal to* $12(8^3 - 4^3)$*) the* $24 \times 24$ *matrix of native unit faces has* 93 *nonzero entries, rank* 24*, is not bipartite, and has 2 connected components.*

The Spectre's edges fall into two classes that never meet within a class, and the chair's faces do not. The boundary operators differ in the same way as the inflations: the supertile perimeter of the Spectre obeys the recurrence with characteristic polynomial $(x-1)(x^2-4x-1)$ of Section 5, and the surface of the chair obeys $S_N = 24 \cdot 4^N$, with characteristic polynomial $x - 4$.

### 9.4 The Hat and the Turtle see their lattice; the Spectre does not

**Computation, not Fact.** The Hat and the Turtle, unlike the Spectre at $(a, b) = (1, 1)$, tile on a hexagonal lattice $\mathbb{C}/\mathbb{Z}[\zeta_3]$, and that can be read in reciprocal space. For the vertex set of a level-5 patch at unit density, with a Gaussian window of width 9, a fraction 0.86 of the Bragg intensity above threshold of the Hat lies within 12% of a point of the dual lattice (from 16 peaks) and 1.00 for the Turtle (from 12 peaks), against 0.00 and 0.00 for the same lattice rotated or rescaled. The Spectre has strong peaks as well, but only a fraction 0.00 of them is on such a lattice (control 0.06, 36 peaks). This is the reciprocal-space form of the statement that Tile$(1, 1)$ is not on the lattice. It is one patch and one window, no exponent is claimed, and it does not bear on the pure-point theorem. For the Spectre the control fraction exceeds the measured one, so this statistic cannot by itself show the absence of a lattice; that statement rests on the vertices spanning the rank-four module $\mathbb{Z}[\zeta_{12}]$ (Fact 15).

## 10 What the substitution hierarchy supplies

**Computation, not Fact.** Whether the level index of a substitution can be read as an arrow, a record, a look-back or a clock is a question that any physical reading of these tilings would

need answered [3]. Four readings are tested on finite patches against controls. The programs are in the `spectre` repository, built on `hierarchy_cache.py`, which walks the substitution tree and keeps each tile's address; the numbers are those they print at build time, and distances are in tile scales $\ell$.

**Clustering.** Barbour, Koslowski and Mercati [19] use a scale-invariant clustering measure of equal-mass points, $C_S = \ell_{\mathrm{rms}}/\ell_{\mathrm{mhl}}$, to identify an arrow of time in the gravitational $N$-body problem. For the tile centroids of the level-$n$ patch $C_S$ is 0.360, 0.539, 0.604, 0.626 for $n = 1, \ldots, 4$, but the rise is the footprint: against a triangular lattice cut to the same outline the excess is 0.028 at $n = 1$ and at most 0.001 for $n = 2, 3, 4$. Positional clustering carries no arrow.

**Records.** How large a neighbourhood must a tile see to name its level-$k$ ancestor? By leave-one-out prediction from the radius-$r$ neighbourhood, the level-1 ancestor is determined at $3\ell$ (error 0.000, against 0.151 at $2\ell$), while the level-2 ancestor is still wrong in 0.446 of cases at $4\ell$ and 0.072 at $8\ell$; at full size the radius grows by about a factor of three per level. Finer levels are free and coarser ones cost a patch three times larger, an asymmetry that is an arrow only if an observer's patch grows in one direction, which the tiling does not supply.

**Look-back.** Let $h$ be the level of the lowest common ancestor of two tiles at distance $d$ (Figure 8). If depth were look-back time, $\langle h \rangle$ would grow as $\log_\lambda d$; it does, with slope 0.92 (0.89 for a quadtree with $\lambda = 2$ through the same code), below 1 because $h$ is capped. For tiles 1 to $2\ell$ apart, $P(h \geq k+1)/P(h \geq k)$ is 0.483, 0.518 for $k = 2, 3$ in the Spectre and 0.525, 0.504 for $k = 3, 4$ in the quadtree. The outline dimension $\ln \nu / \ln \lambda = 1.3993$ would give $\nu/\lambda^2 = 0.538$ and the quadtree 1/2; the data do not separate them, but an exact count does. For tiles sharing an edge, the pairs whose lowest common ancestor has level $\ell$ are the edges between different children of the level-$\ell$ supertiles. Their number in a level-$N$ patch is $T(N - \ell)$ times the glue of (2), which Theorem 1 gives exactly. As $N \to \infty$, $P(h \geq k+1)/P(h \geq k)$ is 0.394, 0.498, 0.528, 0.536 for $k = 1, \ldots, 4$ and tends to $\nu/\lambda^2$. So the tail ratio is $\nu/\lambda^2$, not 1/2. The dictionary holds on average and is shared by any self-similar hierarchy, and spatial neighbours can be several levels apart in it.

**Parity.** The common determinant of the placements in a depth-$n$ patch alternates in sign with $n$ (Proposition 1), so the construction mirrors at every level. Were that a clock, reflection-odd statistics would alternate with level (Figure 9). For tile pairs they do not: the mean of $\sin(\theta_o + \theta_t - 2\phi)$, verified to change sign under a mirror image, for pairs 1 to $3\ell$ apart is 0.25 when the common ancestor is the level-1 supertile and $-0.12$, $-0.14$, $-0.15$ for levels $2, 3, 4$, and the swirl $\langle \sin(\theta - \phi) \rangle$ about a level-$k$ supertile centre is negative at every level ($-0.43$, $-0.21$, $-0.15$ for $k = 1, 2, 3$). In outlines the flip is visible: a level-$k$ supertile outline is nearer to the mirror image of the same-type level-$(k+1)$ one than to a rotation in 24 of 24 comparisons, and nearer to a rotation of the level-$(k+2)$ one in 15 of 15, clearly only for $k = 3$ (0.19 by rotation against 0.37 with reflection). The alternation lives in the shapes of supertiles and not in the tiles; the mirror image of a Spectre tiling is a Spectre tiling, so it belongs to the substitution as written and is not a dynamics.

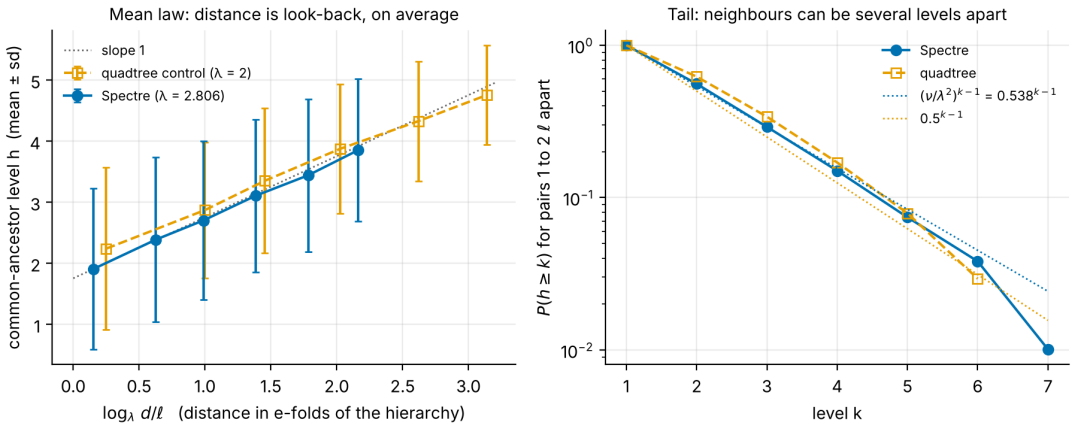


Figure 8: Left: mean common-ancestor level against $\log_\lambda d/\ell$ (with standard deviation), Spectre and quadtree control. Right: the tail $P(h \geq k)$ for pairs 1 to $2\ell$ apart, with $0.538^{k-1}$ and $0.5^{k-1}$.

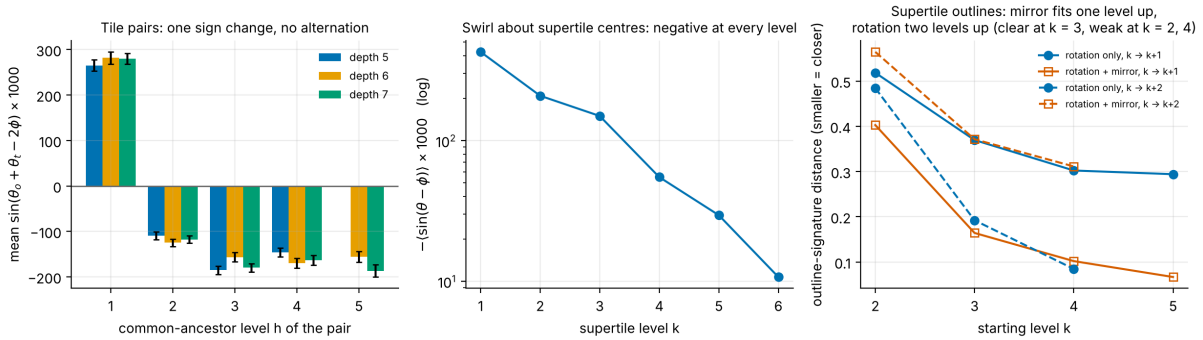


Figure 9: (a) The reflection-odd pair statistic by common-ancestor level, depths 5 to 7. (b) The swirl of tile orientations about supertile centres. (c) Outline-signature distance between same-type supertiles one and two levels apart, by rotation only and with reflection.

**What follows.** Positional clustering shows no excess over its control beyond the first level; the record asymmetry and the look-back dictionary are real but generic; the parity alternation comes from the rule and not from the tile data. None supplies a rule for what propagates, and none supplies a physical clock; what that would mean physically is discussed in the companion note [3], not here. (Figures for the clustering and record computations are in `paper/figures/spectre_hier_clustering` and `spectre_hier_records`.)

## 11 Conclusion

The two tilings separate cleanly in the quantities computed: the Spectre by a unit of $\mathbb{Z}[\sqrt{15}]$, a perimeter growing by a unit of $\mathbb{Q}(\sqrt{5})$ at every order, and an exact internal plane; the Chair44 by inflation 2 on $\mathbb{Z}^3$, no Euclidean internal space, no twist, an explicit pure-point centre set, orientation sums $2^n$ and face contacts that are not bipartite. The main new result is the hull theorem and the classification of the symmetry groups of Chair44 tilings in Section 7.4, conditional on two unrefereed inputs. The hierarchy tests of Section 10 are negative or generic.

What the Facts do not reach is as follows. The Spectre results take the published substitution rule (matrix and placement transforms) as input, and the Chair44 results Tsiokos's solid and substitution. The einstein property and aperiodicity of the Chair44 are Tsiokos's claimed proof, quoted and not checked [4]. The hull theorem and the symmetry classification of Section 7.4 are proved for tilings obeying the 44 contact rules, from Kamenetsky's unique-hierarchy criterion (Lemma 1, its finite certificate checked independently) and from the count of admissible blocks of Lemma 2, which the build of this paper does not repeat but which an independent implementation reproduces; for tilings by the solid they rest in addition on Tsiokos's registration theorem, quoted, audited by the second author (its written steps checked, all of its finite inputs recomputed), and not refereed. The counts of legal blocks and fixed seeds are recomputed. That the Spectre diffraction is pure point is a published theorem and is quoted. The perimeter recurrence of the Spectre, its closed form, the growth bound and the boundary exponent are proved for every order by the finite certificate of Theorem 1, which is independent code. The box dimension of the limiting boundary, Theorem 2, uses in addition the existence of Spectre tilings of the plane [1]. The twist of the Spectre supertile is a limiting statement. The closed form of the orientation constant is identified and not proved, the window dimension (Theorem 3) uses the regularity of the windows from [9], the weighted diffraction of the chair is only numerically consistent with pure point, and the Hat and Turtle diffraction is one patch with one window. The boundary operator governs the perimeter in the aggregate at every order; resolved by species and edge index, on the orders counted, a handful of components obey neither it nor its obvious extensions, while their ratios still approach $\nu$, and the full fine operator is not claimed. The hierarchy results are numerics on finite patches, with controls, and are not Facts.

One problem remains open: a four-dimensional analogue of the chair, Kamenetsky's Problem 9.1 [12]. An independent implementation of his closure test, which reproduces his three-dimensional count (exactly 3 of the 2187 homochiral assignments close, with $30 \to 44 \to 44$ contacts), was run on 12,784 further four-dimensional assignments. Half of them extend the three-dimensional marking on a facet, and half are random. None is coarsening-closed, and every one exceeds 400 contact poses. A simulated-annealing search on Kamenetsky's statistic $|\Sigma(P_0)|$, which in three dimensions is minimised exactly by the closed assignments (44), made about 12,100 further evaluations. It got below his structured-family plateau of 1566, to 273, but never near a closed value; the question stays open.

# Declarations

## Funding and Competing Interests

The authors received no specific funding for this work, and declare no competing interests.

## Code and Data Availability

All source code and data supporting this study are available at:
https://github.com/brentharts/spectre/
https://github.com/brentharts/spectre-monotile-py/
https://github.com/brentharts/six-birds-tiles/

# References

[1] D. Smith, J.S. Myers, C.S. Kaplan and C. Goodman-Strauss. (2024). *An aperiodic monotile*. Combinatorial Theory, 4(1); arXiv:2303.10798.

[2] D. Smith, J.S. Myers, C.S. Kaplan and C. Goodman-Strauss. (2024). *A chiral aperiodic monotile*. Combinatorial Theory, 4(2); arXiv:2305.17743.

[3] B. Hartshorn and T. Romanov, *A flat initial surface? A speculative reading of the Spectre and Chair44 tilings*, companion note (2026), `spectre_bigbang_note.tex` in https://github.com/brentharts/spectre.

[4] I. Tsiokos (2026). *A strongly aperiodic monotile in three dimensions*, arXiv:2609.19214. Code and data: https://github.com/ioannist/six-birds-tiles (CC BY 4.0).

[5] C. Goodman-Strauss (2026). *Notes on a strongly aperiodic monotile in $E^3$*, arXiv:2609.24779.

[6] F. Flicker (2026). *Matching rules for a three-dimensional strongly aperiodic monotile*, arXiv:2609.23783.

[7] T. Romanov (2026). *The hull and the symmetry groups of Chair44 tilings*, draft. The computations are `chair44_vertex_blocks.py`, `chair44_hull_prune.py` and `chair44_symmetry_census.py`, run on commit `d53d224` of [4] and merged into six-birds-tiles, `verify/hull`; an independent implementation, the reproduction of Kamenetsky's finite conditions, the $O$-orbit certificate of the lemma (`c44lemma_cert.py`, `lemmaA_orbits.json`) and the audit of Tsiokos's registration theorem (`registration_audit.py`, `REGISTRATION_AUDIT.md`) are in the directory `chair44_independent` of this repository.

[8] M. Baake, F. Gähler, J. Mazáč and A. Mitchell, *Diffraction of the Hat and Spectre tilings and some of their relatives*, arXiv:2502.03268.

[9] M. Baake, F. Gähler, J. Mazáč and L. Sadun, *On the long-range order of the Spectre tilings*, Discrete Comput. Geom. **78** (2026) 739–762; arXiv:2411.15503.

[10] M. Baake, F. Gähler and L. Sadun, *Dynamics and topology of the Hat family of tilings*, Israel J. Math. **270** (2025) 449–485; arXiv:2305.05639.

[11] A. Chéritat and N. Ma (initial idea N. Ma; contributions P. Mostert), *4D lift of the tilings by the Smith et al. aperiodic monotile* (2023). https://www.math.univ-toulouse.fr/~cheritat/2023-monotile/4D-lift/

[12] D. Kamenetsky, *Towards Strongly Aperiodic Monotiles in Higher Dimensions*, arXiv:2610.00916.

[13] J.-Y. Lee and R. V. Moody (2001). Lattice substitution systems and model sets. *Discrete Comput. Geom.* 25, 173–201.

[14] M. Baake, R. V. Moody and M. Schlottmann (1998). Limit-(quasi)periodic point sets as quasicrystals with $p$-adic internal spaces. *J. Phys. A: Math. Gen.* 31, 5755–5765.

[15] E. A. Robinson, Jr. (1999). On the table and the chair. *Indag. Math. (N.S.)* 10, 581–599.

[16] A. O. Gelfond (1934). Sur le septième problème de Hilbert. *Izv. Akad. Nauk SSSR* 7, 623–630; Th. Schneider (1935). Transzendenzuntersuchungen periodischer Funktionen I. *J. Reine Angew. Math.* 172, 65–69.

[17] M. Schlottmann (2000). Generalized model sets and dynamical systems. In *Directions in Mathematical Quasicrystals*, CRM Monograph Series 13, AMS, 143–159.

[18] J.-Y. Lee, R. V. Moody and B. Solomyak (2003). Consequences of pure point diffraction spectra for multiset substitution systems. *Discrete Comput. Geom.* 29, 525–560.

[19] J. Barbour, T. Koslowski and F. Mercati, *Identification of a gravitational arrow of time*, Phys. Rev. Lett. **113**, 181101 (2014); arXiv:1409.0917. https://doi.org/10.1103/PhysRevLett.113.181101